

## 1            **Dissolved Inorganic Nutrients in the Western Mediterranean Sea (2004-2017)**

2            Malek Belgacem<sup>1,2</sup>, Jacopo Chiggiato<sup>1,\*</sup>, Mireno Borghini<sup>1</sup>, Bruno Pavoni<sup>2</sup>, Gabriella Cerrati<sup>3</sup>,  
3            Francesco Aciri<sup>1</sup>, Stefano Cozzi<sup>4</sup>, Alberto Ribotti<sup>5</sup>, Marta Álvarez<sup>6</sup>, Siv K. Lauvset<sup>7</sup>, Katrin Schroeder<sup>1</sup>

4            <sup>1</sup> CNR-ISMAR, Arsenale Tesa 104, Castello 2737/F, 30122 Venezia, Italy

5            <sup>2</sup> Dipartimento di Scienze Ambientali Informatica e Statistica, Università Ca' Foscari Venezia,  
6            Campus Scientifico Mestre, Italy

7            <sup>3</sup> ENEA, Department of Sustainability, S. Teresa, Marine Environmental center, 19032 Pozzuolo di  
8            Lerici (SP), Italy

9            <sup>4</sup> CNR-ISMAR, Area Science Park – Basovizza, 34149 Trieste, Italy

10           <sup>5</sup> CNR-IAS, Loc. Sa Mardini snc, Torregrande, 9170 Oristano, Italy

11           <sup>6</sup> Instituto Español de Oceanografía, IEO, A Coruña, Spain

12           <sup>7</sup> NORCE Norwegian Research Centre, Bjerknes Centre for Climate Research, 5007 Bergen, Norway

13           \*Corresponding author's email: [jacopo.chiggiato@ismar.cnr.it](mailto:jacopo.chiggiato@ismar.cnr.it)

### 15           **Abstract**

16           Long-term time-series are a fundamental prerequisite to understand and detect climate shifts and  
17           trends. Understanding the complex interplay of changing ocean variables and the biological  
18           implication for marine ecosystems requires extensive data collection for monitoring, hypothesis testing  
19           and validation of modelling products. In marginal seas, such as the Mediterranean Sea, there are still  
20           monitoring gaps, both in time and in space. To contribute to filling these gaps, an extensive dataset of  
21           dissolved inorganic nutrient observations (nitrate, phosphate,  $\text{Si}$  and silicate) has been collected  
22           between 2004 and 2017 in the Western Mediterranean Sea and subjected to rigorous quality control  
23           techniques to provide to the scientific community a publicly available, long-term, quality controlled,  
24           internally consistent biogeochemical data product. The data product includes 870 stations of dissolved  
25           inorganic nutrients, including temperature and salinity, sampled during 24 cruises. Details of the  
26           quality control (primary and secondary quality control) applied are reported. The data are available in  
27           PANGAEA (<https://doi.org/10.1594/PANGAEA.904172>, Belgacem et al. 2019)

28 **Keywords:** Mediterranean Sea, Dissolved Inorganic Nutrient, biogeochemistry.

29

## 30 **1 Introduction**

31 Dissolved inorganic nutrients play a crucial role in marine ecosystem functioning. They serve as  
32 regulators of ocean biological productivity, and are trace elements for biogeochemical cycling as well  
33 as for natural and anthropogenic sources and transport processes (Bethoux, 1989; Bethoux et al.,  
34 1992). They are also non-conservative tracers, since their distribution vary according to both  
35 biological (such as primary production and respiration) and physical (such as convection, advection,  
36 mixing and diffusion) processes. Very schematically, inorganic nutrients are continuously consumed  
37 by phytoplankton (due to primary production) in the sea surface and regenerated in the mesopelagic  
38 layer by bacteria and animals (due to respiration). Moreover, the sinking of organic matter and its  
39 decomposition increases the nutrient concentrations in the intermediate and deep-water masses over  
40 time. To identify the limiting factors for biological production in the oceans, we need to understand  
41 the underlying chemical constraints and especially the macro- and micronutrients spatial and temporal  
42 variations. Dissolved inorganic nutrients may be used as tracers of water masses like salinity and  
43 temperature, to assess mixing processes, and to understand the biogeochemical circumstances of their  
44 formation regions. Understanding the complex interplay of changing ocean variables and the  
45 biological implication for marine ecosystems is a difficult task and requires not only modelling, but  
46 also extensive data collection for monitoring, hypothesis testing and validation. Monitoring gaps still  
47 remain in both in time and space, especially for marginal seas such as the Arctic Ocean or the  
48 Mediterranean Sea.

49 The Mediterranean Sea has been identified as a region significantly affected by ongoing climatic  
50 changes, like warming and decrease in precipitation (Giorgi, 2006). In addition, it is a region  
51 particularly valuable for climate change research because it behaves like a miniature ocean (Bethoux

52 et al., 1999) with a well-defined overturning circulation characterized by spatial and temporal scales  
53 much shorter than for the global ocean, with a turnover of only several decades. Being an  
54 intercontinental sea, and subjected to more terrestrial nutrient inputs (river runoff, submarine  
55 groundwater discharge) and atmospheric deposition, the Mediterranean Sea has a nitrate to phosphate  
56 N:P ratio that is anomalously high compared to the “classical” world's oceans Redfield ratio,  
57 indicating a general P-limitation regime, which becomes stronger along a west-to-east gradient. The  
58 Mediterranean Sea is therefore a potential model to study global patterns that will be experienced in  
59 the next decades worldwide, not only regarding ocean circulation, but also the marine biota (Lejeune  
60 et al., 2010). Several environmental variables can act as stressors for marine ecosystems, by which  
61 climatically driven ecosystem disturbances are generated (Boyd, 2011). These changes affect, among  
62 others, the distribution of biogeochemical elements (including inorganic nutrients) and the functioning  
63 of the biological pump and CO<sub>2</sub> regulation.

64 Within this context, the aim of this paper is to compile an extensive dataset of dissolved inorganic  
65 nutrient observations (nitrate, phosphate, and silicate) collected between 2004 and 2017 in the  
66 Western Mediterranean Sea (WMED), to describe the quality control techniques and to provide the  
67 scientific community with a publicly available, long-term, quality controlled, and internally consistent  
68 biogeochemical data product, contributing to previously published Mediterranean Sea datasets like the  
69 MEDAR/Medatlas (time period:1908–1999), (Fichaut et al., 2003) and the Mediterranean Sea –  
70 Eutrophication and Ocean Acidification aggregated datasets v2018 (time period: 1911-2017) provided  
71 by EMODnet Chemistry (Giorgetti al.,2018) available at  
72 <https://www.seadatanet.org/Products/Aggregated-datasets>.

73 Both original and quality-controlled data are available in PANGAEA:

74 <https://doi.org/10.1594/PANGAEA.904172>Coverage: 44°N-35°S; 6°W-14°E

75 Location Name: Western Mediterranean Sea

76 Date start: May 2004

77 Date end: November 2017

## 78 **2 Dissolved inorganic nutrient data collection**

### 79 **2.1. The CNR dissolved inorganic nutrient data in the WMED**

80 Long-term time-series, such as the OceanSites global time series ([www.oceansites.org](http://www.oceansites.org)), are a  
81 fundamental prerequisite to understand and detect climate shifts and trends. However, biogeochemical  
82 time-series are still limited to the northern Western Mediterranean Sea (MOOSE network, Coppola et  
83 al., 2019). Yet, inorganic nutrients in the Mediterranean Sea has received more attention in recent  
84 years, and various datasets have been compiled to understand its unique characteristics such as the one  
85 build by the PERSEUS project Consortium (“Policy-oriented marine environmental research in the  
86 southern European seas” - EU FP7 project GA #287600), that included 100 cruises collected during  
87 the project’s lifetime, in addition to those from other projects like SESAME, EU FP7 project GA  
88 #GOCE-036949), and data products such as the MEDAR/Medatlas. In addition to that, the data  
89 assembly system EMODnet Chemistry, a leading infrastructure supported by pan-European directorate  
90 General MARE set up (Martin Miguez et al., 2019, Tintoré et al., 2019).

91 The dataset presented here consists of 24 oceanographic cruises (Fig. 1, Table 1a and Table 1b)  
92 conducted in the WMED on board of research vessels run by the Italian National Research Council  
93 (CNR) and the Science and Technology Organisation Centre for Maritime Research and  
94 Experimentation (NATO-STO CMRE). All cruises were merged into a unified dataset with 870  
95 nutrient stations and ~ 9666 data points over a period of 13 years (2004-2017). The overall spatial  
96 distribution of the stations covers the whole WMED, but the actual distribution strongly varies  
97 depending on the specific cruise and most of the data are collected along sections. At all stations,  
98 pressure, salinity and temperature were measured with a CTD-rosette system consisting of a CTD SBE  
99 911 plus and a General Oceanics rosette with 24 12L Niskin Bottles. Temperature measurements were  
100 performed with the SBE-3/F thermometer with a resolution of  $10^{-3}$  °C; conductivity measurements

101 were performed with the SBE-4 sensor with a resolution of  $3 \cdot 10^{-4}$  S/m. The probes were calibrated  
102 before and after each cruise. During all CNR cruises, redundant sensors were used for both  
103 temperature and salinity measurements.

104 Seawater samples for dissolved inorganic nutrient measurements were collected during the CTD up-  
105 cast at standard depths (with slight modifications according to the depth at which the deep chlorophyll  
106 maximum was detected). The standard depths are usually 5, 25, 50, 75, 100, 200, 300, 400, 500, 750,  
107 1000, 1250, 1500, 1750, 2000, 2250, 2500, 2750, 3000 m. No filtration was employed, nutrient  
108 samples were immediately stored at  $-20$  °C. Note that sample storage and freezing duration varied  
109 greatly from one cruise to another (Table 3 shows cruises where this exceeded 1 year).

## 110 **2.2. Analytical methods for inorganic nutrients**

111 For all cruises, nutrient determination (nitrate, orthosilicate and orthophosphate) was carried out  
112 following standard colorimetric methods of seawater analysis, defined by Grasshoff et al. (1999) and  
113 Hansen and Koroleff (1999). For inorganic phosphate, the method is based on the reaction of the ions  
114 with an acidified molybdate reagent to yield a phosphomolybdate heteropoly acid, which is then  
115 reduced to a blue-colored compound (absorbance measured at 880 nm). Inorganic nitrate is reduced  
116 (with cadmium granules) to nitrite that react with an aromatic amine leading to the final formation of  
117 the azo dye (measured at 550 nm). Then, the nitrite separately determined must be subtracted from the  
118 total amount measured to get the nitrate concentration only. The determination of dissolved silicon is  
119 based on the formation of a yellow silicomolybdic acid reduced with ascorbic acid to blue-colored  
120 complex (measured at 820 nm).

121 Nutrient analysis was performed in three laboratories. From 2004 to 2013, all cruises nutrients were  
122 analysed by ENEA, while for those of 2015 (cruise #23) and 2017 (cruise #24), nutrient  
123 concentrations were analysed by CNR-ISMAR. Referring to Table 1S, four different models of  
124 autoanalyzer were used. Measurements from the autoanalyzer were reported in  $\mu\text{mol L}^{-1}$ . Inorganic

125 nutrient concentrations were converted to the standard unit  $\mu\text{mol kg}^{-1}$ , using sample salinity from CTD  
126 and a mean laboratory analytical temperature of 20°C. Data from nutrient analysis were then merged  
127 to ancillary CTD bottle data.

### 128 **2.3. Reference inorganic nutrient data**

129 In addition to the data collected during the above-mentioned cruises, and in order to perform the  
130 secondary quality control (described below), we identified five reference cruises (Table 2), based on  
131 their spatial and temporal distribution and the reliability of the measurements (see Fig. 2 –Table.3S  
132 Fig.1S). Cruises 06MT20110405 and 06MT20011018 are the only two Mediterranean cruises included  
133 in the publicly available Global Ocean Data Analysis Project version 2 (GLODAPv2, Olsen et al.  
134 2016). These cruises, conducted on board the R/V Meteor, provide a reliable reference because  
135 nutrient analysis strictly followed the recommendation of the World Ocean circulation experiment  
136 (WOCE) and the GO-SHIP protocols (Hydes et al., 2010; ,Tanhua et al., 2013). Cruises  
137 29AH20140426 and 48UR20070528 are to be included in the CARIMED data product (personal  
138 communication by M. Álvarez, in preparation but not yet available) and have undergone rigorous  
139 quality control following GLODAP routines. Finally, 29AJ20160818 was carried out in the framework  
140 of the MedSHIP programme (Schroeder et al., 2015) and its data are available at  
141 <https://doi.org/10.1594/PANGAEA.902293> (Tanhua, 2019).

### 142 **3 Quality Assurance and quality control methods**

143 Combining inorganic nutrient data from different sources, collected by different operators, stored for  
144 different amounts of time, and analysed by multiple laboratories, is not a straightforward task. This is  
145 widely recognized in the biogeochemical oceanographic community. Since the 1990s, several studies  
146 and programmes (e.g. World Ocean Database, World Ocean Atlas, WOCE) have been devoted to  
147 facilitate the exchange of oceanographic data and develop quality control procedures to compile  
148 databases by the estimation of systematic errors (Gouretski and Jancke, 2000) to increase the inter-  
149 comparability, generate consistent data sets and accurately observe the long-term change.

150 An example of a first quality control procedure is the use of reference materials that are available for  
151 salinity (IAPSO, salinity standard by OSIL) and temperature (SPRT, Standard Platinum Resistance  
152 Thermometer). As for the inorganic carbon, total alkalinity (Dickson et al., 2003) and inorganic  
153 nutrients (Aoyama et al., 2016), certified reference materials (CRM) have been recently made  
154 applicable for oceanographic cruises. However, since CRM are not always available or used for  
155 biogeochemical oceanographic data, Lauvset and Tanhua (2015) developed a secondary quality  
156 control tool to identify biases in deep data. The method suggests adjustments that reduce cruise to  
157 cruise biases, increase accuracy and allow for the inter-comparison between data from various sources.  
158 This approach, based on a crossover and inversion method (Gouretski and Jancke, 2000; Johnson et  
159 al., 2001), was used to generate the CARbon IN Atlantic ocean (CARINA, see Hoppema et al., 2009),  
160 GLODAPv2.2019 (Olsen et al., 2019) and PACIFICA (Suzuki al al.,2013) data products.

### 161 **3.1 Primary Quality control**

162 Each individual cruise was first subjected to a primary quality control (1<sup>st</sup> QC) that included a check of  
163 apparent and extreme outliers in CTD salinity, nitrate, phosphate and silicate. Each parameter included  
164 a quality control flag, following standard WOCE flags (Table 3). Surface, intermediate and deep layer  
165 were evaluated separately because nutrient observations evolve differently in each layer. The  
166 coefficient of variation (CV, defined as standard deviation over mean) was computed for each depth  
167 layer. Coefficients of variation in the surface (0-250 db) layer were high (nitrate CV=1.16, phosphate  
168 CV=1.005, silicate CV=0.75) due to air-sea interaction (Muniz et al., 2001) occurring in this layer  
169 rendering it difficult to flag. These influences are of reduced importance in the intermediate (250-1000  
170 db) layer (nitrate CV=0.23, phosphate CV=0.31, silicate CV=0.24) and the deep (>1000 db) layer  
171 (nitrate CV=0.15, phosphate CV=0.22, silicate CV=0.14), decreasing the total variance. Flags in the  
172 upper and intermediate layer were thus set based on outliers within pressure ranges defined according  
173 to standard pressures (0-10, 10-30, 30-60, 60-80, 80-160, 160-260, 260-360, 360-460, 460-560, 560-  
174 1000 db).

175 Below 1000 db, flagging included an inspection of nitrate to phosphate (N:P) and nitrate to silicate (N:  
176 Si) ratios. The Median and Median Absolute Deviation (MAD) was computed by classes of pressure:  
177 we considered as outlier any atypical observation and any value that departs from the median by more  
178 than three MADs in the different pressure ranges for each cruise.

179 An overview of the nutrient distribution is provided with scatter plots, showing also the flagged  
180 measurements (Fig. 3). Each measurement was flagged 2 (“Acceptable/ measured”) or flagged 3  
181 (“Questionable”): 4.1% of nitrate data, 3.37% of phosphate data, 3.16% of silicate data, and 0.07% of  
182 CTD salinity data were considered outliers and flagged 3. As highlighted by Tanhua et al. (2010), the  
183 primary QC can be subjective depending on the expertise of the person flagging the data, thus flagging  
184 could bring in some uncertainties.

185 In order to have a first assessment of the precision of each cruise measurements, the standard deviation  
186 of observations deeper than 1000 db was calculated along with averages and standard deviations for  
187 each cruise and by subregions to have an overview about nutrient content variability in the deep layer  
188 and about the observations spatial spread of individual cruises (Table 4). Following the subdivision of  
189 Manca et al. (2004), the WMED has been divided into subregions (Fig.2S, Table 2S) according to the  
190 general circulation patterns (details in Manca et al.,2004). Table 4 displays the comparison of standard  
191 deviation of deep measurements for each cruise and within subregions. The overall standard deviation  
192 between cruises in the deep layer varied between 0.51 and 1.41  $\mu\text{mol kg}^{-1}$  for nitrate, between 0.1 and  
193 1.64  $\mu\text{mol kg}^{-1}$  for silicate and between 0.025 and 0.078  $\mu\text{mol kg}^{-1}$  for phosphate. Regional standard  
194 deviation of nitrate measurements below 1000 db varied between 0.08  $\mu\text{mol kg}^{-1}$  in the Gulf of Lion  
195 (DF2) with cruise #9 and 1.6  $\mu\text{mol kg}^{-1}$  in the Balearic Sea (DS2) observations of cruise #14.  
196 Phosphate lowest regional standard deviation was 0.01  $\mu\text{mol kg}^{-1}$  found in the observations of cruise  
197 #9 in Gulf of Lion (DF2), cruise #10 in Balearic Sea (DS2) and Algerian West (DS3), cruise #14 and  
198 cruise # 15 in Tyrrhenian South (DT3), cruise #18 in Algero-Provençal (DF1) and Sardinia Channel  
199 (DI1) while the highest standard deviation was 0.1  $\mu\text{mol kg}^{-1}$  in the observations of cruise #12 in



200 Algerian West (DS3). As for silicate, the lowest standard deviation was  $0.02 \mu\text{mol kg}^{-1}$  observed in  
201 cruise #9 measurements of Gulf of Lion subregion (DF2) and the highest deep standard deviation was  
202 observed in cruise #6 in its all subregions together with cruise #5 measurement in Tyrrhenian North  
203 (DT1) with  $1.83 \mu\text{mol kg}^{-1}$  standard deviation.

204 Cruises #3, #6 and #9 had the largest spatial extension (see right side of Fig. 9) with a high number of  
205 samples over more than seven subregions (Table 4), the geographical variability of the distribution in  
206 dissolved inorganic nutrients results thus in the largest standard deviations. Conversely, cruises with  
207 smaller spatial coverages have lower standard deviations. Therefore, a relatively small spatial  
208 coverage and high standard deviation is considered as indicative of data with low precision (Olsen et  
209 al., 2016). This applies to cruises #1, #5, and #16. Despite the small spatial coverage, samples of  
210 nitrate and phosphate of cruise #5 have an overall standard deviation of  $1.35 \mu\text{mol kg}^{-1}$  and  $0.07 \mu\text{mol}$   
211  $\text{kg}^{-1}$ , respectively, a high standard deviation pointed out also in the regional standard deviation of deep  
212 measurements in Tyrrhenian North (DT1) and South (DT3) . Cruise #1, with few stations in  
213 Tyrrhenian North (DT1) and South (DT3) subregions and 21 samples below 1000 db, has an overall  
214 standard deviation of  $1.25 \mu\text{mol kg}^{-1}$  for nitrate,  $0.06 \mu\text{mol kg}^{-1}$  for phosphate and  $1.64 \mu\text{mol kg}^{-1}$  for  
215 silicate. The regional standard deviation was relatively high for nitrate ( $0.51\text{-}1.32 \mu\text{mol kg}^{-1}$ ),  
216 phosphate ( $0.02\text{-}0.065 \mu\text{mol kg}^{-1}$ ) and silicate ( $0.53\text{-}1.83 \mu\text{mol kg}^{-1}$ ). A comparison with the deviations  
217 from e.g. cruise # 2, carried out in the same year and e.g. cruise #17 (with a similar cruise track),  
218 confirms the lower precision of the data of cruise #1. Similar considerations apply to the quality of  
219 nitrate samples ( $0.87\text{-}1.02 \mu\text{mol kg}^{-1}$ ) and silicate ( $0.87\text{-}0.9 \mu\text{mol kg}^{-1}$ ) from cruise #16, covering a  
220 small area in Tyrrhenian North (DT1) and South (DT3), compared to cruise #17, carried out in the  
221 same regions (right side of Fig. 9 and Table 4).

222 Deep silicate measurements of cruise #6 have twice the overall standard deviation of silicate data of  
223 cruise #8 from the same year. Adding to that, in the seven subregions, the regional standard deviation  
224 of deep silicate observations was the highest, between  $1.04\text{-}2 \mu\text{mol kg}^{-1}$  which was relatively high

225 compared to the surrounding cruises that have observations in the same subregions. This is again  
226 suggestive of the limited precision. On the other hand, trying to explain the source of relatively high  
227 standard deviations in specific cruises is not always straightforward, as they could stem from a variety  
228 of sources, sampling, conservation and analysis. The bottom water in the WMED exhibits a high  
229 nutrient content below 1000 db (Table 4), due to the longer residence time. Dividing the WMED into  
230 subregions, has effectively removed the natural spatial change in nutrients, making the interpretation  
231 of the standard deviation a matter of the precision of the measurements only.

232 In Table 4, deep averages by subregions showed that overall nutrient concentration fluctuated around  
233  $7.4 \pm 0.9 \mu\text{mol kg}^{-1}$  for nitrate,  $0.3 \pm 0.06 \mu\text{mol kg}^{-1}$  for phosphate and  $7.7 \pm 0.8 \mu\text{mol kg}^{-1}$  for silicate,  
234 similar findings were reported by Manca et al. (2004). Comparing cruise averages in each region  
235 enabled the identification of “suspect” cruises. Cruise #24 has the lowest deep average in nitrate in  
236 Algero-Provençal (DF1), Tyrrhenian North (DT1) subregions and Sardinia Channel (DI1). As for  
237 silicate of cruises #24 and #16 was very low compared to the overall regional average in Liguro-  
238 Provençal (DF3) and Tyrrhenian South (DT3) subregions. Deep average of phosphate did not show  
239 any outlier cruises in all subregions. Different reasons could explain the low precision in the samples,  
240 freezing is one. Although it is a valid preservation method (Dore et al., 1996), the error is higher when  
241 samples were not analysed immediately (Segura-Noguera et al., 2011), so the storage time could  
242 influence.

### 243 **3.2 Secondary Quality control: the crossover analysis**

244 The method used to perform the secondary QC on the WMED dissolved inorganic nutrient dataset  
245 makes use of the quality-controlled reference data, and the crossover analysis toolbox developed by  
246 Tanhua (2010a) and Lauvset and Tanhua (2015). The computational approach is based on comparing  
247 the cruise data set to a high-quality reference data set to quantify biases, described in detail in Tanhua  
248 et al. (2010b). Here, we summarize the technique with emphasis on inorganic nutrients. The first step  
249 consisted of selecting reference data, as described in section 2.3. The second step is the crossover

250 analysis that was carried out using a MATLAB Toolbox (available online: <https://cdiac.ess->  
251 [dive.lbl.gov/ftp/oceans/2nd\\_QC\\_Tool\\_V2/](https://cdiac.ess-dive.lbl.gov/ftp/oceans/2nd_QC_Tool_V2/)) where crossovers are generated as difference between two  
252 cruises using the “running cluster” crossover routine. Each cruise is thus compared to the chosen set of  
253 reference cruises. For each crossover, samples deeper than 1000 db are selected within a predefined  
254 maximum distance set to 2°arc distance, defined as a crossing region, to ensure the quality of the  
255 offset with a minimum number of crossovers and to minimize the effect of the spatial change. The  
256 reason to select measurements deeper than 1000 db, is to remove the high frequency variability  
257 associated to mesoscale features, biological activity and the atmospheric forcing acting in the upper  
258 layers, that might induce changes in biogeochemical properties of water masses. On the other hand,  
259 also the deep Mediterranean cannot be considered truly “unaffected” by changes, as it is intermittently  
260 subjected to ventilation (Schroeder et al., 2016; Testor et al., 2018) and the real variability can be  
261 altered in adjusting data. The computational approach takes this into account, since weights are given  
262 to the less variant profile in the crossing region, according to the “confidence” in the determined offset  
263 of the compared profiles (i.e. the weighted mean offset of a given crossover-pair is weighted to the  
264 depth where the offsets of all compared profiles have the smallest variation which indeed is strongly  
265 interlinked with the degree of variance of each profile) (for further details see Lauvset and Tanhua,  
266 2015).

267 Before identifying crossovers, each profile was interpolated using the piecewise cubic Hermite method  
268 and the distance criteria outlined in Lauvset and Tanhua (2015), their Table 1a, detailed in Key et al.  
269 (2004). The crossover is a comparison between each interpolated profile of the cruise being evaluated  
270 and the interpolated profile of the reference cruise. The result is a weighted offset (defined as  
271 difference cruise/reference) and a standard deviation of the offset. The standard deviation is indicative  
272 of the precision; however, it is important to note that this assumption only works because it is a  
273 comparison to a reference, and the absolute offset is indicative of accuracy.

274 The third step consists in evaluating and selecting the suggested correction factor that was applied to  
275 the whole water column. The correction factor was calculated from the weighted mean offset of all  
276 crossovers found between the cruise and the reference data set, involving a somewhat subjective  
277 process.

278 For inorganic nutrients, offsets are multiplicative so that a weighted mean offset > 1 means that the  
279 measurements of the corresponding cruise are higher than the measurements of the reference cruise in  
280 the crossing region and applying the adjustment would decrease the measured values. The magnitude  
281 of an increase or a decrease is the difference of the weighted offset from 1. In general, no adjustment  
282 smaller than 2% (accuracy limit for nutrient measurements) is applied (detailed description is found in  
283 Hoppema et al., 2009; Lauvset and Tanhua, 2015; Olsen et al., 2016; Sabine et al., 2010; Tanhua et al.,  
284 2010b).

285 The last step is the computation of the weighted mean (WM) to determine the internal consistency and  
286 quantify the overall accuracy of the adjusted product (Hoppema et al., 2009; Sabine et al., 2010;  
287 Tanhua et al., 2009), with the difference that our assessment is based on the offsets with respect to a  
288 set of reference cruises. This WM reflects the absolute weighted mean offset of the data set compared  
289 to the reference data set, hence the smaller the WM the higher the internal consistency. The accuracy  
290 was computed from the individual absolute weighted offsets. The WM, which will be discussed in  
291 section 4.4., was computed using the individual weighted absolute offset (D) of number of crossovers  
292 (L) and the standard deviation ( $\sigma$ ):  $WM = \frac{\sum_{i=1}^L D(i)/(\sigma(i))^2}{\sum_{i=1}^L 1/(\sigma(i))^2}$

#### 293 **4 Results of the secondary QC and recommendations**

294 The results of the secondary QC revealed the necessary corrections for nitrate, phosphate and silicate.  
295 Four cruises were not considered in the crossover analysis: cruises #7 and #11 do not have enough  
296 stations > 1000 db (at least 3 to get valid statistics), while cruises #19 and #21 were outside the spatial  
297 coverage of the reference cruises. Cruises that were not used for the crossover analysis are made

298 available in the original dataset but were not included in the final data product (see Supplementary  
299 material – Part 2 (A2)).

300 Overall, we found a total number of 73 individual crossovers for nitrate, 72 for phosphate and 54 for  
301 silicate. An example of the running cluster crossover output is shown in Fig.4. Results of the crossover  
302 analysis is an adjustment factor for each cruise and each nutrient, that are shown in Table 5 and Fig. 5-  
303 6-7. The adjustment factor was calculated from the weighted mean of absolute offset summarized in  
304 Table 6 and Fig. 3S-4S-5S. Table 6 details the improvement of the weighted mean of absolute offset  
305 by cruise prior to and after adjustments, the information is also displayed graphically in Fig. 3S-4S-5S.  
306 Cruises are in chronological order in all figures and tables.

#### 307 **4.1 Nitrate**

308 The crossover analysis suggests a significant adjustment for nitrate concentrations on 15 cruises,  
309 between 0.94 and 0.98 (for adjustments  $<1$ ) and between 1.02 and 1.34 (for adjustments  $>1$ ) (Table 5  
310 and Fig.5). Offsets suggest that the deep measurements of cruises #1, #3, #4, #5, #6, #8, #12, #13, #15,  
311 #16, #23 and #24 need to be adjusted towards higher concentrations, when compared to the respective  
312 reference (Fig.3S).

313 Nitrate observations of cruises #2, #9 and #10 on the other hand were higher than the reference cruises  
314 and exhibit variation outside the accepted accuracy limit, thus require a downward adjustment.

315 Finally, five cruises (#14, #17, #18, #20, and #22) were consistent with the reference data and no  
316 adjustment was necessary. Considering the weighted mean of absolute offset after adjustments shown  
317 in Table 6, two cruises (#5 and #24) required large correction factors but remain outside the accuracy  
318 threshold (Fig. 5). These cruises are considered in detail later (section 4.4).

#### 319 **4.2 Phosphate**

320 For phosphate the crossover analysis suggests adjustments for 20 cruises, as shown in Fig. 6. Deep  
321 phosphate measurements of 15 cruises (Table 6) appear to be lower than the respective reference  
322 measurements (i.e. phosphate data of these cruises require an upward adjustment), while the data of  
323 five cruises (#2, #3, #4, #6, #24) are higher (i.e. they need a downward adjustment) (Fig.4S). Applying  
324 all the indicated adjustments, the large offsets of cruises #2, #3, #4, #6, #8, #9, #10, #18, #20, #23 and  
325 #24 are reduced and became consistent with the reference. Cruises #1, #5, #12, #13, #14, #15, #16,  
326 #17, and #22 retain an offset even after applying the indicated adjustment. These cruises are  
327 considered in detail later.

328 According to Olsen et al. (2016), if a temporal trend is detected in the offsets, no adjustments should  
329 be applied. There is indeed a decreasing trend between 2008 and 2017 in the phosphate correction  
330 factor (Fig. 6), and thus an increasing one in the weighted mean offset (Fig.4S), implying a temporal  
331 increase of phosphate. Therefore, phosphate data of the cruises being part of the trend were not  
332 flagged as questionable, except some cruises that are discussed further in section 4.4.

333 Comparing phosphate before and after adjustment, the corrections did minimise the difference with the  
334 reference, while the actual variation with time was preserved (Fig.6). The temporal trend towards  
335 higher phosphate concentrations in the Mediterranean Sea is considered to be real, even though  
336 studies concerning the biogeochemical trends in the deep layers of the WMED are scarce (Pasqueron  
337 et al., 2015). However, this variation could be consistent with the findings of Béthoux et al.(1998,  
338 2002) and the modelling studies by Moon et al. (2016) and Powley et al. (2018) who indeed found an  
339 increasing trend in phosphate concentrations over time, due to the increase in the atmospheric and  
340 terrestrial inputs.

### 341 **4.3 Silicate**

342 The results of the crossover analysis for silicate suggests corrections for all cruises (Fig.7). The  
343 crossovers indicate that deep silicate measurements are lower in the evaluated cruises than in the

344 corresponding reference cruises (i.e. they need to be adjusted upward) (Fig.5S). This is likely to be a  
345 direct result of freezing the samples before analysis, since the reactive silica polymerizes when frozen  
346 (Becker et al., 2019). After applying the adjustment (Table 5), as expected, the offsets are reduced  
347 (Table 6), but five cruises (#1, #5, #6, #15, and #16) remain outside the accuracy envelope. Due to the  
348 large offsets, these cruises will be discussed further in section 4.4.

#### 349 **4.4 Discussion and recommendation**

350 Adjustments were evaluated for each cruise separately. As a general rule, no correction was applied  
351 when the suggested adjustment is strictly within the 2% limit (indicated with NA in Table 5). The  
352 average correction factors were 1.06 for nitrate, 1.14 for phosphate and 1.14 for silicate, respectively.  
353 To verify the results, we re-ran the crossover analysis and re-computed offsets and adjustment factors  
354 using the adjusted data (as shown in blue in Fig. 3S-4S-5S and Fig. 5-6-7). Most of the new  
355 adjustments are within the accuracy envelope and few are outside the limit, except for the cruises  
356 belonging to the above mentioned “phosphate-trend” and the other outlying cruises which are detailed  
357 hereafter. By the application of adjustments, the deep-water offsets were reduced. This can be seen in  
358 the decrease of the weighted mean offset between the data before adjustments (after 1<sup>st</sup> QC, Fig. 3S-  
359 4S-5S, in grey) and the adjusted data (after 2<sup>nd</sup> QC, Fig. 3S-4S-5S, in blue).

360 Referring to the analysis detailed in section 3.2, the internal consistency of the nutrient data set has  
361 improved and increased significantly after the adjustment, from 4% for nitrate, 19% for phosphate and  
362 13% for silicate, to a more unified dataset with 3 % for nitrate, 6 % for phosphate and 3% for silicate.

363 A comparison between the original and the adjusted nutrient observations is shown in Fig. 8A-B-C,  
364 indicating an improvement in the accuracy based on the reference data and a relatively reduced range  
365 particularly for phosphate (Fig. 8B). Figure 8. D-E scatterplots show that after the quality control,  
366 nutrient stoichiometry slopes obtained from regressions, between tracers along the water column  
367 demonstrate a strong coupling and provide a nitrate to phosphate ratio of ~22.09 and a nitrate to

368 silicate ratio of ~0.94. These values are consistent with nutrient ratios range found in the WMED as  
369 reported in Lazzari et al. (2016); Pujo-Pay et al., (2011) and Segura-Noguera et al. (2016). The  
370 regression model is more accurate after adjustments with an improved  $r^2$  for N:P (from 0.81 to 0.90)  
371 and for N: Si (from 0.85 to 0.87).

372

373 In the following some details on the adjustment of specific cruises are given:

374 Cruise #2 [48UR20041006] needed an adjustment of 0.98 for nitrate, 0.9 for phosphate and 1.06 for  
375 silicate. Most of the crossover profiles occur in the Tyrrhenian Sea (Tyrrhenian North and Tyrrhenian  
376 South subregions). After adjustment, the cruise is inside the 2% envelope.

377 Cruise #3 [48UR20050412] appeared to be outside the 2% envelope before adjustments. Its offsets  
378 with five reference cruises, crossing the Tyrrhenian Sea, Sardinia Channel, Gulf of Lion and Algero-  
379 Provençal subregions, showed that nitrate and silicate values to be relatively low, and thus an  
380 adjustment of 1.08 and 1.15 was applied respectively. On the other hand, phosphate values were  
381 relatively high, and a 0.93 adjustment was applied.

382 Cruise #4 [48UR20050529] correction factor estimate was based on five crossovers that covered five  
383 subregions: Tyrrhenian South, Sardinian Channel, Algerian East and West and the Alboran Sea. Table  
384 4 show that there are no large differences between regional averages within the cruise which justify an  
385 adjustment of 1.04 for nitrate, 0.85 for phosphate and 1.183 for silicate.

386 Cruise #8 [48UR20060928] was adjusted by 1.03 for nitrate, 1.14 for phosphate and 1.1 for silicate,  
387 because it showed values to be low compared to four references. After adjustment, the data were  
388 inside the acceptable range.

389 Cruise #9 [48UR20071005] values of nitrate were slightly outside the 2% envelope before  
390 adjustments, similar to phosphate and silicate that were lower compared to the reference. The



391 adjustments of 0.97 for nitrate, 1.14 for phosphate and 1.115 for silicate suggested by the mean offset  
392 against the reference cruises were recommended.

393 Cruise #13 [48UR20090508] has three crossovers in the common crossing zone that included  
394 Tyrrhenian North, Tyrrhenian South and Sardinia Channel subregions. The crossover suggests that this  
395 cruise has too low values and needs an adjustment of 1.05 for nitrate, 1.33 for phosphate and 1.15 for  
396 silicate.

397 Cruise #14 [48UR20100430] has a mean offset with four reference cruises that suggests an adjustment  
398 factor of 1.34 for phosphate and 1.123 for silicate. Nitrate did fall within the accuracy envelope; no  
399 adjustment was needed.

400 Cruise #10 [48UR20080318] has only three crossovers in the Algero-Provençal subregion, showing  
401 that nitrate is too high compared to the reference while phosphate and silicate are slightly lower. We  
402 therefore applied the adjustments of Table 5, since the deep averages in each region (Table 4) did not  
403 show large regional difference.

404 Cruise #17 [48UR20110421] crossover analysis did not suggest any correction for nitrate; however,  
405 with an offset based on two crossovers in the Tyrrhenian North and South subregions, adjustments  
406 were recommended for phosphate (1.25) and silicate (1.12), for being lower than the reference cruises.

407 Cruise #18 [48UR20111109] is similar to cruise #17, since it was suggested to adjust phosphate by  
408 1.14 and silicate by 1.09, based on four crossovers in the Tyrrhenian North and South, Sardinia  
409 Channel and Algero-Provençal subregions.

410 Cruise #20 [48UR20120111] has four crossovers over the Tyrrhenian North and South and Algero-  
411 Provençal subregions. Its measurements were slightly lower than the reference cruises suggesting a  
412 correction factor of 1.17 for phosphate and 1.08 for silicate.

413 Cruise #22 [48UR20131015] has similar correction factors as cruise #20, based on three crossovers in  
414 the Sardinia Channel and Tyrrhenian North and South subregion, with measurements being lower than  
415 the reference.

416 Cruise #23 [48QL20150804] showed nutrient values slightly lower than the reference cruises as well,  
417 suggesting small correction factors of 1.02 for both nitrate and phosphate and 1.08 for silicate, a  
418 correction factors that were based on offsets with five cruises.

419 Below, we discuss the recommended flags in the final product (Table 3; see supplementary Materials  
420 Part-2 (A2)) assigned for some cruises that needed further consideration, since they required larger  
421 adjustment factors:

422 Cruise #1 [48UR20040526]: The adjusted values are still lower than the reference (Fig.5-6-7-Fig.3S-  
423 4S-5S) and are still outside the 2% accuracy range. This cruise had stations in the Sicily Strait,  
424 Tyrrhenian North and South and Ligurian East subregions (Fig. 9, right side) and only 4 stations were  
425 deeper than 1000 db (those within the Tyrrhenian Sea). The low precision of this cruise has already  
426 been evidenced during the 1<sup>st</sup> QC (section 3.1). We recommend flagging this cruise as questionable  
427 (flag 3).

428 Cruise #5 [48UR20051116]: This cruise took place between Sicily Strait and the Tyrrhenian North and  
429 South (Fig. 9, right side). Nitrate, phosphate and silicate data were lower than those from other cruises  
430 (#3 and #4) run the same year (Fig. 5-6-7-Fig.3S-4S-5S) and are still biased after adjustments.  
431 Considering the limited precision and the low number of crossovers, it is recommended to flag the  
432 cruise as questionable (flag 3).

433 Cruise #6 [48UR20060608]: This cruise had an offset with five cruises giving evidence that  
434 adjustments of 1.05 for nitrate, 0.86 for phosphate and 1.26 for silicate are needed. The silicate bias  
435 was reduced after adjustment but remained large with respect to the accuracy limit (Fig. 7-Fig. 5S).  
436 This cruise has a wide geographic coverage, with stations along 9 sections (Fig. 9, right side).

437 Considering also the high standard deviation (Table 4), which is partially attributed to the spatial  
438 coverage of the cruise, there is still uncertainty about the quality of the samples. It is recommended to  
439 flag silicate data of cruise #6 as questionable (flag 3).

440 Cruise #12 [48UR20081103]: Phosphate data have low accuracy with respect to the reference cruises  
441 (Fig. 6-Fig. 4S). This cruise has stations along a longitudinal section from Sicily Strait to the Alboran  
442 Sea, which might explain the large standard deviation of deep phosphate samples (Table 4). Cruise  
443 #12 was given a correction of 1.08 for nitrate, 1.12 for silicate and 1.38 for phosphate. The mean  
444 offset from five crossovers computed within the Tyrrhenian South, Sardinia Channel, Algerian East,  
445 Algerian West and Alboran Sea subregions suggests that this cruise has lower nutrient values than the  
446 reference cruise. After adjustment, cruise #12 is within the acceptable range for nitrate and silicate but  
447 not for phosphate as highlighted in section 3.2. In addition, considering the relatively high number of  
448 stations >1000 db and a plausible trend in phosphate, it is recommended to flag the phosphate data as  
449 good/acceptable (flag 2).

450 Cruise #15 [48UR20100731]: This cruise has 149 station along a similar track as cruise #12 but shows  
451 larger offsets for phosphate and silicate (Fig. 6-7-Fig. 4S-5S), compared to cruise #12. Considering  
452 that deep silicate data was not of low quality (small standard deviation, see Table 4), and that deep  
453 phosphate fall within the “phosphate-trend” discussed above, these data are flagged good/acceptable  
454 (flag 2).

455 Cruise #16 [48UR20101123]: The cruise shows large offsets for phosphate and silicate (Fig. 6-7- Fig.  
456 4S-5S), similar to cruise #15. Considering that the overall cruise standard deviation of silicate samples  
457 below 1000 db was relatively high (1.02 over 14 samples, see Table 4), and that it has only one  
458 crossover between the Tyrrhenian North and South subregions (Table 6), and that when comparing  
459 deep regional averages, this cruise had the lowest average silicate value, it is recommended to flag  
460 silicate data of cruise #16 as questionable (flag 3). As for phosphate, the cruise is part of the  
461 “phosphate-trend” and is therefore flagged good/acceptable (flag 2).

462 Cruise #24 [48QL20171023]: This cruise has the largest offset for nitrate even after adjustment. It is  
463 very likely due to a difference between laboratories (calibration standards) concerning nitrate, which  
464 needs to be flagged as questionable (flag 3) in the final product.

465 There are several sources of bias in the observation. One of the main reasons for an upward/  
466 downward bias would be the difference in the nutrient's chemical analytical method and the lack of  
467 use of CRM in all cruises as also noted in CARINA (Tanhua et al., 2009) or in the most recent global  
468 comparability study by Aoyama (2020).

469 Cruises discussed in this section were not removed from the final product but are retained along with  
470 their recommended quality flag (Table 3) detailed above and in the supplementary material – Part 2  
471 (A2)). We have done the evaluation of their overall quality but leave it up to the users how to  
472 appropriately use these data.

#### 473 **4.5 Product assessment: Comparison with MEDATLAS**

474 Averages water mass biogeochemical properties have been computed from the adjusted product (Table  
475 7), and compared to the MEDAR/Medatlas annual climatological profiles, downloaded from the  
476 Italian NODC website (<http://doga.ogs.trieste.it/medar/>) given by Manca et al. (2004), in order to  
477 evaluate and asses the new product. Since nutrient properties exhibit differences with depths, we  
478 compared average nutrient concentrations of the three main water masses in twelve subregions of the  
479 WMED (Table 7, Fig 2S).

480 The results of Table 7 compares water mass biogeochemical properties with the reference climatology.  
481 The new product agrees well with the Medatlas climatology. However, there are some distinctions.  
482 The surface layer (0-150db) is characterized by a low nutrient content. The surface nitrate varies  
483 between 0.69 and 2.75  $\mu\text{mol kg}^{-1}$  with a maximum found in the Ligurian East (DF4) and the minimum  
484 in the Alboran Sea (DS1) subregions, similar values were recorded in the climatology (0.61- 3.00  
485  $\mu\text{mol kg}^{-1}$ ). The differences in nitrate averages in the surface layer are observed in the Gulf of Lion

486 (DF2) where the new product is higher than the climatology and slightly lower in the Liguro-  
487 Provençal (DF3). As for, the surface content in phosphate, it varied between 0.04 and 0.16  $\mu\text{mol kg}^{-1}$   
488 with a maximum found in the Ligurian East (DF1) and a minimum in the Alboran Sea (DS1), alike the  
489 Medatlas climatology, where phosphate averages fluctuate between 0.05 and 0.19  $\mu\text{mol kg}^{-1}$ . The new  
490 product is slightly lower compared to the climatology. As to the average surface in silicate, it varies  
491 between 1.36 and 2.91  $\mu\text{mol kg}^{-1}$  with a minimum found in the Ligurian East (DF4), the maximum in  
492 the Gulf of Lion (DF2)) while in the climatology, it varied between 1.27 and 2.31  $\mu\text{mol kg}^{-1}$  (the  
493 minimum in the Ligurian East (DF4) and the maximum in the Alboran Sea (DS1)). The new product is  
494 slightly higher in silicate.

495 Overall, the differences in the surface layer are observed in the Gulf of Lion (DF2), the Liguro-  
496 Provençal (DF3) and the Ligurian East (DF4) regions which could be due to the intense variability of  
497 the vertical mixing occurring in the northern WMED compared to the other subregions.

498 In the intermediate layer, averages were computed from the depth of the salinity maximum ( $S_{\text{max}}$ )  
499  $\pm 100\text{m}$  from a regional average profile, indicative of the Levantine Intermediate Water (LIW) core.  
500 Nitrate average varied between 4.94 and 9.32  $\mu\text{mol kg}^{-1}$  where the minimum content was recorded in  
501 Sicily strait (DI3) and the maximum in the Algerian West (DS3) while in the Medatlas climatology,  
502 nitrate was between 5.14 and 8.60  $\mu\text{mol kg}^{-1}$ . In average, the lowest content in nitrate was in the  
503 Tyrrhenian North (DT1) and South (DT3), Sardinia Channel (DI1) and Sicily Strait (DI3) while LIW  
504 of the Gulf of Lion (DF2), Liguro-Provençal (DF3), Ligurian East (DF4), Balearic Sea (DS2), Algero-  
505 Provençal (DF1), Alboran Sea (DS1), Algerian West (DS3) and East (DS4) subregions was relatively  
506 rich in nitrate. Compared to the Medatlas product, though the new product was slightly higher mainly  
507 in the Gulf of Lion (DF2), Ligurian East (DF4) and Balearic Sea (DS2). As for phosphate, LIW  
508 averages showed similar behavior as nitrate, the lowest phosphate content (0.21- 0.27  $\mu\text{mol kg}^{-1}$ ) was  
509 observed in the Eastern subregions of WMED (DI3, DI1, DT3 and DT1), when the maximum  
510 concentrations (0.4-0.37  $\mu\text{mol kg}^{-1}$ ) were reported in the Western subregions of the WMED (DS1, DS3

511 and DS4, DS2 and DF2). The large differences between the two products were in the Ligurian East  
512 (DF4) and the Alboran Sea (DS1), subregions of few numbers of observations.

513 Concerning silicate, the lowest average concentration ( $5.25 \mu\text{mol kg}^{-1}$ ) was observed in LIW core of  
514 Sicily Strait (DI3,) and the maximum concentrations ( $8.66 - 8.77 \mu\text{mol kg}^{-1}$ ) were in the Alboran Sea  
515 (DS1) and Gulf of Lion (DF2), similar values were recorded in the Medatlas climatology ( $4.86-7.95$   
516  $\mu\text{mol kg}^{-1}$ ). There are some discrepancies, where the new product was higher particularly in the Gulf  
517 of Lion (DF2), Liguro-Provençal (DF3) and Algerian West (DS3) subregions. This difference is  
518 explained by the limited number of observations within depth range in the new product compared to  
519 the observations used in the climatology in these subregions.

520 Referring to Manca et al.,(2004), the LIW core salinity values are relatively more pronounced in Sicily  
521 Strait (DI3), Sardinia Channel (DI1) and in the Tyrrhenian South (DT3) and North (DT1) subregions,  
522 where nutrients were lower than the Western subregions (DS3, DS4, DS1 , DF1, DS2, DF4, DF3,  
523 DF2). The averages of nutrient within the LIW core ties well with the Medatlas climatology averages  
524 (Table 7), except in subregions with important vertical mixing.

525 We have verified also average biochemical properties in the deep layer (below 1500db). The new  
526 product is slightly higher in nitrate averages ( $7.74 - 8.37 \mu\text{mol kg}^{-1}$ ) than the Medatlas climatology  
527 ( $7.12 - 8.06 \mu\text{mol kg}^{-1}$ ) (Table 7). The largest difference was found in Tyrrhenian South (DT3) and  
528 North (DT1) subregions. This difference could be due to the fact that, we are comparing two different  
529 time periods (2004-2017 and 1908-2001). As for the deep layer phosphate, average concentrations  
530 varied between  $0.35$  and  $0.37 \mu\text{mol kg}^{-1}$  and were within the climatology limits ( $0.31 - 0.40 \mu\text{mol kg}^{-1}$ ).  
531 In all subregions, there was not large differences. Overall, phosphate was in accordance with the  
532 Medatlas climatology. Similar to nitrate, deep average silicate in the new product ( $8.64 - 9.21 \mu\text{mol kg}^{-1}$ )  
533 was higher than the climatology ( $7.51$  to  $9.04 \mu\text{mol kg}^{-1}$ ). The largest difference in average silicate  
534 was observed in the Tyrrhenian North (DT1), South (DT3) and Liguro-Provençal (DF3) subregions.

535 We then used the Root Mean Squared Error (RMSE) as statistical index to quantify the difference  
536 between averaged regional profiles from the new product and Medatlas product. The climatology  
537 annual profiles were interpolated to the regional average profiles of the new product, and the average  
538 RMSE for each layer and subregion was calculated. Fig. 10 shows the regional evolution of RMSE in  
539 the main water masses for the three nutrients. For nitrate (Fig. 10 A), the RMSE in the surface layer  
540 varied between  $0.12 \mu\text{mol kg}^{-1}$  (in the Tyrrhenian North (DT1)) and  $1.36 \mu\text{mol kg}^{-1}$  (in the Gulf of  
541 Lion (DF2)); in the intermediate layer, the RMSE was between  $0.07 \mu\text{mol kg}^{-1}$  (in the Sardinia  
542 Channel (DI1)) and  $2.35 \mu\text{mol kg}^{-1}$  (in the Gulf of Lion (DF2)), and was lower in the deep layer,  
543 between  $0.11 \mu\text{mol kg}^{-1}$  (in the Algerian East (DS4)) and  $0.79 \mu\text{mol kg}^{-1}$  (the Gulf of Lion (DF2)). The  
544 RMSE decreases in the Algerian East (DS4), Tyrrhenian North (DT1), Tyrrhenian South (DT3),  
545 Sardinia Channel (DI1) and Sicily Strait (DI3). This illustrates the low difference between the two  
546 products.

547 For phosphate (Fig. 10 B), the RMSE ranges between  $0.0022 \mu\text{mol kg}^{-1}$  (in the Tyrrhenian South  
548 (DT3)) and  $0.12 \mu\text{mol kg}^{-1}$  (in the Ligurian East (DF4)) in the surface layer; and is between  $0.003$   
549  $\mu\text{mol kg}^{-1}$  (in the Liguro-Provençal subregion (DF3)) and  $0.048 \mu\text{mol kg}^{-1}$  (in the Alboran Sea (DS1))  
550 at intermediate depths, while in the deep layer RMSE varied between  $0.0087$  (in the Gulf of Lion  
551 (DF2)) and  $0.057 \mu\text{mol kg}^{-1}$  (in the Tyrrhenian North (DT1)).

552 Regarding silicate RMSE (Fig. 10 C) in surface, it varied between  $0.13 \mu\text{mol kg}^{-1}$  (in the Algero-  
553 Provençal subregion (DF1)) and  $3.5 \mu\text{mol kg}^{-1}$  (in the Ligurian East subregion (DF4)), A lower RMSE  
554 between  $0.10 \mu\text{mol kg}^{-1}$  (in the Sardinia Channel (DI1)) and  $2.54 \mu\text{mol kg}^{-1}$  (in the Gulf of Lion (DF2))  
555 was reported in the intermediate layer; the results in deep layer, were between  $0.33 \mu\text{mol kg}^{-1}$  (in the  
556 Algerian East (DS4)) and  $1.43 \mu\text{mol kg}^{-1}$  (in the Liguro-Provençal subregion (DF3)).

557 The best agreement between the two products was observed in the intermediate and deep layer. The  
558 lowest RMSE was confined to the deep layer in most of the subregions while the highest difference  
559 was found in the surface layer since it is subjected to intense vertical mixing mainly in the northern

560 WMED. Comparing averages in subregions, showed similar differences in nutrient between the two  
561 products particularly in the Gulf of Lion (DF2), the Liguro-Provençal (DF3), Ligurian East (DF4) and  
562 Algerian East (DS4), due to the relative high variability in nutrient concentrations in these subregions.  
563 These differences are not significant as there is discrepancy on the number of observations used in the  
564 two products. Overall, inorganic nutrients of the new product agree very well with the  
565 MEDAR/Medatlas climatology. The main features of the spatial distribution in the inorganic nutrients  
566 were in accordance with the findings of Manca et al., (2004), where the relative high content in  
567 nutrient was found in the intermediate layer of the Algerian subregions (DF1, DS3, DS4) than in other  
568 subregions ( Table 7). Besides, the highest concentrations in deep layer silicate were reported in the  
569 Algerian subregions in the two products ( $9.21 \mu\text{mol kg}^{-1}$  (DS3) in the new product;  $9.04 \mu\text{mol kg}^{-1}$   
570 (DS4) in the climatology), which is indicative of the poor regional ventilation and of the longer  
571 residence time of deep water especially in these subregions.

## 572 **5 Final remarks**

573 An internally consistent data set of dissolved inorganic nutrients has been generated for the WMED  
574 (2004-2017). The accuracy envelope for nitrate and silicate was set to 2%, a predefined limit used in  
575 GLODAP and CARINA data products. Regarding phosphate data, these were almost entirely outside  
576 this limit, because of its natural variations and the overall very low concentrations in the WMED, a  
577 highly P-limited basin. Using a crossover analysis (2<sup>nd</sup> QC toolbox) to compare cruises with respect to  
578 reliable reference data, improved the accuracy of the measurements by bias-minimizing the individual  
579 cruises. The new product was broadly in consistent with the earlier climatology MEDAR/Medatlas.

580 The publication of a quality-controlled extensive (spatially and temporally) database of inorganic  
581 nutrients in the WMED was timely and fills a gap in information that prevented baseline assessments  
582 on spatial and temporal variability of biogeochemical tracers in the Mediterranean. In combination  
583 with older databases in the same region (e.g. bottle data available in the MEDAR/Medatlas database),  
584 this new data producte will thus constitute a pillar on which the Mediterranean marine scientific



585 community will be able to build on original research topics on biogeochemical fluxes and cycles and  
586 their relation to hydrological changes that occurred in the period covered by the dataset. The dataset is  
587 also relevant for the modelling community as it can be used as an independent data product to assess  
588 reanalysis products or it can be assimilated in new reanalysis products.

## 589 **6 Data availability**

590 The final product is available as a .csv merged file from PANGAEA, and can be accessed at  
591 <https://doi.org/10.1594/PANGAEA.904172> (Belgacem et al. 2019).

592 Ancillary information is in the supplementary materials with the list of variables included in the  
593 original and final product. Table 1a and Table 1b summarizes all cruises included in the dataset. The  
594 dataset include frequently measured stations and key transects of the WMED with in situ physical and  
595 chemical oceanographic observations. As mentioned, two files are accessible, both include  
596 oceanographic variables observed at the standard depths (see supplementary Materials Part-2).

597 - *Original dataset: CNR\_DIN\_WMED\_20042017\_original.csv*: This is the original dataset with  
598 flag variable for each of the following parameter: CTD salinity, nitrate, phosphate and silicate  
599 from the primary quality control (detailed in section 3.1).

600 - *Adjusted dataset: CNR\_DIN\_WMED\_20042017\_adjusted.csv*: This is the product after  
601 primary quality control and after applying the adjustment factors from the secondary quality  
602 control. Recommendations of section 4.4 are included, as well as quality flags.

603 **Author contribution:** MB, MA, SL, JC and KS substantially contributed to write the manuscript. SC,  
604 GC and FA run the chemical analysis and contributed to the manuscript. MB coordinated the technical  
605 aspects of most of the cruises. SC, GC, FA, AR, BP contributed in specific part of the manuscript.

606 **Acknowledgements.** The data have been collected in the framework of several of national and  
607 European projects, e.g.: KM3NeT, EU GA #011937; SESAME, EU GA #GOCE-036949; PERSEUS,

608 EU GA #287600; OCEAN-CERTAIN, EU GA #603773; COMMON SENSE, EU GA #228344;  
609 EUROFLEETS, EU GA #228344; EUROFLEETS2, EU GA # 312762; JERICO, EU GA #262584;  
610 the Italian PRIN 2007 program “Tyrrhenian Seamounts ecosystems”, and the Italian RITMARE  
611 Flagship Project, both funded by the Italian Ministry of University and Research. We thank Sarah  
612 Jutterström from the Swedish Environmental Research institute for the invaluable help in Quality  
613 Control discussions. We would like to express our appreciation to the INOCEN laboratory team at  
614 IEO for their help and collaboration during MB’s stay there. The authors are deeply indebted to all  
615 investigators and analysts who contributed to data collection at sea during so many years, as well as to  
616 the PIs of the cruises (S. Aliani, M. Astraldi, M. Azzaro, M. Dibitto, G. P. Gasparini, A. Griffa, J.  
617 Haun, L. Jullion, G. La Spada, E. Manini, A. Perilli, C. Santinelli, S. Sparnocchia), the captains and  
618 the crews for allowing the collection of this enormous dataset; without them, this work would not have  
619 been possible.

620

621

622

623

624

625

626

627

628

629

630  
631  
632  
633  
634  
635  
636

637 **References**Aoyama, M., Woodward, E., Malcolm, S., Bakker, K., Becker, S., Björkman, K., Daniel,  
638 A., Mahaffey, C., Murata, A., Naik, H., Tanhua, T., Rho, T., Roman, R. and Sloyan, B.: Comparability  
639 of oceanic nutrient data, Poster Cluster Community Whitepaper, CLIVAR Open Science Conference  
640 on "Charting the course for climate and ocean research", 18-25 September 2016, Qingdao (China), 12  
641 pp., <http://hdl.handle.net/10261/17137>, 2016.

642 Aoyama, M.: Global certified-reference-material-or reference-material-scaled nutrient gridded dataset  
643 GND13. *Earth System Science Data*, 12, 487-499, <https://doi.org/10.5194/essd-12-487-2020>, 2020.

644 Becker, S., Aoyama, M., Woodward, E.M.S., Bakker, K., Coverly, S., Mahaffey, C., and Tanhua, T.:  
645 GO-SHIP Repeat Hydrography Nutrient Manual: The precise and accurate determination of dissolved  
646 inorganic nutrients in seawater, using Continuous Flow Analysis methods, In: *The GO-SHIP Repeat  
647 Hydrography Manual: A Collection of Expert Reports and Guidelines*, 56 ,  
648 <http://dx.doi.org/10.25607/OBP-555>, 2019.

649  
650 Belgacem, M., Chiggiato, J., Borghini, M., Pavoni, B., Cerrati, G., Acri, F; Cozzi, S., Ribotti, A.,  
651 Álvarez, M., Lauvset, S. K., Schroeder, K.: Quality controlled dataset of dissolved inorganic nutrients  
652 in the western Mediterranean Sea (2004-2017) from R/V oceanographic cruises. *PANGAEA*,  
653 <https://doi.org/10.1594/PANGAEA.904172>, 2019.

654 Bethoux, J. P.: Oxygen consumption, new production, vertical advection and environmental evolution  
655 in the Mediterranean Sea, *Deep Sea Research, Part A, Oceanographic Research Papers*, 36(5), 769–  
656 781, doi:10.1016/0198-0149(89)90150-7, 1989.

657 Bethoux, J. P., Morin, P., Madec, C. and Gentili, B.: Phosphorus and nitrogen behaviour in the  
658 Mediterranean Sea, *Deep Sea Research, Part A, Oceanographic Research Paper*, 39(9), 1641–1654,  
659 doi:10.1016/0198-0149(92)90053-V, 1992.

660 Bethoux, J. P., Gentili, B., Morin, P., Nicolas, E., Pierre, C. and Ruiz-Pino, D.: The Mediterranean

661 Sea : a miniature ocean for climatic and environmental studies and a key for the climatic functioning of  
662 the North Atlantic, *Progress in Oceanography*, 44, 131–146, 1999.

663 Béthoux, J. P., Morin, P., Chaumery, C., Connan, O., Gentili, B. and Ruiz-Pino, D.: Nutrients in the  
664 Mediterranean Sea, mass balance and statistical analysis of concentrations with respect to  
665 environmental change, *Marine Chemistry*, 63(1–2), 155–169, doi:10.1016/S0304-4203(98)00059-0,  
666 1998.

667 Béthoux, J. P., Morin, P. and Ruiz-Pino, D. P.: Temporal trends in nutrient ratios: Chemical evidence  
668 of Mediterranean ecosystem changes driven by human activity, *Deep Sea Research Part II Topical  
669 Studies in Oceanography*, 49(11), 2007–2016, doi:10.1016/S0967-0645(02)00024-3, 2002.

670 Boyd, P. W.: Beyond ocean acidification, *Nature Geoscience*, 4(5), 273–274, doi:10.1038/ngeo1150,  
671 2011.

672 Coppola, L., Raimbault, P., Mortier, L., and Testor, P.: Monitoring the environment in the  
673 northwestern Mediterranean Sea, *Eos*, 100, <https://doi.org/10.1029/2019EO125951>, 2019.

674 Dickson, A. G., Afghan, J. D. and Anderson, G. C.: Reference materials for oceanic CO<sub>2</sub> analysis: A  
675 method for the certification of total alkalinity, *Marine Chemistry*, 80(2–3), 185–197,  
676 doi:10.1016/S0304-4203(02)00133-0, 2003.

677 Dore, J. E., Houlihan, T., Hebel, D. V., Tien, G., Tupas, L., Karl, D. M.: Freezing as a method of  
678 sample preservation for the analysis of dissolved inorganic nutrients in seawater, *Marine  
679 Chemistry*, 53(3-4), 173-185, 1996.

680 Fichaut, M., Garcia, M. J., Giorgetti, A., Iona, A., Kuznetsov, A., Rixen, M. and Group, M.:  
681 MEDAR/MEDATLAS 2002: A Mediterranean and Black Sea database for operational oceanography,  
682 Elsevier Oceanography Series, 69, 645–648, doi:10.1016/S0422-9894(03)80107-1, 2003.

683 Giorgetti, A., Partescano, E., Barth, A., Buga, L., Gatti, J., Giorgi, G., Iona A., Lipizer, M.,  
684 Holdsworth, N., Larsen, M.M., Schaap, D., Vinci, M., Wenzer, M. :EMODnet Chemistry Spatial Data  
685 Infrastructure for marine observations and related information. *Ocean & Coastal Management*, 166, 9-  
686 17, 2018.Giorgi, F.: Climate change hot-spots, *Geophysical Research Letters*, 33(8), 1–4,  
687 doi:10.1029/2006GL025734, 2006.

688 Gouretski, V. V. and Jancke, K.: Systematic errors as the cause for an apparent deep water property  
689 variability: Global analysis of the WOCE and historical hydrographic data, *Progress in Oceanography*,  
690 48(4), 337–402, doi:10.1016/S0079-6611(00)00049-5, 2000.

691 Grasshoff, K., Kremling K., Ehrhardt M.: *Methods of seawater analysis* (3rd ed.), Weinheim  
692 Press, WILEY-VCH, 203-273, 1999.

693 Hansen, H. P. and Koroleff, F.: Determination of nutrients, *Methods of Seawater Analysis*, 159–228,  
694 1999.

695 Hoppema, M., Velo, A., van Heuven, S., Tanhua, T., Key, R. M., Lin, X., Bakker, D. C. E., Perez, F.  
696 F., Ríos, A. F., Lo Monaco, C., Sabine, C. L., Álvarez, M. and Bellerby, R. G. J.: Consistency of  
697 cruise data of the CARINA database in the Atlantic sector of the Southern Ocean, *Earth System*

698 Science Data, 1(1), 63–75, doi:10.5194/essd-1-63-2009, 2009.

699 Hydes, D. J., Aoyama, M., Aminot, A., Bakker, K., Becker, S., Coverly, S., Daniel, A., Dickson, A. G.,  
700 Grosso, O., Kerouel, R., van Ooijen, J., Sato, K., Tanhua, T., Woodward, E. M. S. and Zhang, J. Z.  
701 :Determination of Dissolved Nutrients (N, P, SI) in Seawater With High Precision and Inter-  
702 Comparability Using Gas-Segmented Continuous Flow Analysers. In: The GO-SHIP Repeat  
703 Hydrography Manual: A Collection of Expert Reports and Guidelines. Version 1. (eds Hood, E.M.,  
704 C.L. Sabine, and B.M. Sloyan). IOCCP Report Number 14, ICPO Publication Series Number 134. 87  
705 pp., <http://dx.doi.org/10.25607/OBP-555>, 2010.

706

707 Johnson, G. C., Robbins, P. E. and Hufford, G. E.: Systematic adjustments of hydrographic sections  
708 for internal consistency, *Journal of Atmospheric Oceanic Technology*, 18(7), 1234–1244,  
709 doi:10.1175/1520-0426(2001)018<1234:SAOHSF>2.0.CO;2, 2001.

710 Key, R. M., Kozyr, A., Sabine, C. L., Lee, K., Wanninkhof, R., Bullister, J. L., Feely, R. A., Millero,  
711 F. J., Mordy, C. and Peng, T. H.: A global ocean carbon climatology: Results from Global Data  
712 Analysis Project (GLODAP), *Global Biogeochem. Cycles*, 18(4), 1–23, doi:10.1029/2004GB002247,  
713 2004.

714 Lauvset, S. K. and Tanhua, T.: A toolbox for secondary quality control on ocean chemistry and  
715 hydrographic data, *Limnology and Oceanography Methods*, 13(11), 601–608,  
716 doi:10.1002/lom3.10050, 2015.

717 Lazzari, P., Solidoro, C., Salon, S. and Bolzon, G.: Spatial variability of phosphate and nitrate in the  
718 Mediterranean Sea: A modeling approach, *Deep Sea Research Part I*, 108, 39–52,  
719 doi:10.1016/j.dsr.2015.12.006, 2016.

720 Lejeusne, C., Chevaldonné, P., Pergent-Martini, C., Boudouresque, C. F. and Pérez, T.: Climate  
721 change effects on a miniature ocean: the highly diverse, highly impacted Mediterranean Sea, *Trends in*  
722 *Ecology and Evolution*, 25(4), 250–260, doi:10.1016/j.tree.2009.10.009, 2010.

723 Manca, B., Burca, M., Giorgetti, A., Coatanoan, C., Garcia, M. J., and Iona, A. : Physical and  
724 biochemical averaged vertical profiles in the Mediterranean regions: an important tool to trace the  
725 climatology of water masses and to validate incoming data from operational oceanography. *Journal of*  
726 *Marine Systems*, 48(1-4), 83-116, 2004.

727 Martín Míguez, B., Novellino, A., Vinci, M., Claus, S., Calewaert, J. B., Vallius, H., Schmitt, T.,  
728 Pititto, P., Giorgetti, A., Askew, N., Iona, S., Schaap, D., Pinardi, N., Harpham, Q., Kater, B.J.,  
729 Populus, J., She, J., Vasilev Palazov, A., McMeel, O., Oset, P., Lear, D., Manzella, G.M.R., Goringe,  
730 P., Simoncelli, S., Larkin, K., Holdsworth, N., Dimitrios\_Arvanitidis C., Molina-Jack M.E., Chaves-  
731 Montero M.D.M. , Herman, P.M.J., and Hernandez F.: The European marine observation and data  
732 network (EMODnet): visions and roles of the gateway to marine data in Europe. *Frontiers in Marine*  
733 *Science*, 6, 2019.

734 Moon, J., Lee, K., Tanhua, T., Kress, N. and Kim, I.: Temporal nutrient dynamics in the  
735 Mediterranean Sea in response to anthropogenic inputs, , 5243–5251,  
736 doi:10.1002/2016GL068788. Received, 2016.

737 Muniz, K., Cruzado, A., Ruiz De Villa, C. and Villa, C. R. De: Statistical analysis of nutrient data  
738 quality ( nitrate and phosphate ), applied to useful predictor models in the northwestern Mediterranean  
739 Sea, *Methodology*, 17, 221–231, 2001.

740 Olsen, A., Key, R. M., Heuven, S. Van, Lauvset, S. K., Velo, A., Lin, X., Schirnack, C., Kozyr, A.,  
741 Tanhua, T., Hoppema, M. and Jutterström, S.: The Global Ocean Data Analysis Project version 2 (   
742 GLODAPv2 ) – an internally consistent data product for the world ocean, , 297–323,  
743 doi:10.5194/essd-8-297-2016, 2016.

744 Olsen, A., Lange, N., Key, R., Tanhua, T., Alvarez, M. et al.: GLODAPv2.2019 -an update of  
745 GLODAPv2. *Earth Syst. Sci. Data*, 11 (3), pp.1437 - 1461. ff10.5194/essd-11-1437-2019ff. fhal-  
746 02315662, 2019.

747 Pasqueron, O., Fommervault, D., Migon, C., Ortenzio, F. D., Ribera, M. and Coppola, L.: Temporal  
748 variability of nutrient concentrations in the northwestern Mediterranean sea ( DYFAMED time-series  
749 station ), *Deep. Res. Part I*, 100, 1–12, doi:10.1016/j.dsr.2015.02.006, 2015.

750 Powley, H. R., Krom, M. D. and Van Cappellen, P.: Phosphorus and nitrogen trajectories in the  
751 Mediterranean Sea (1950–2030): Diagnosing basin-wide anthropogenic nutrient enrichment, *Progress  
752 in Oceanography*, 162, 257–270, doi:10.1016/j.pocean.2018.03.003, 2018.

753 Pujo-Pay, M., Conan, P., Oriol, L., Cornet-Barthaux, V., Falco, C., Ghiglione, J. F., Goyet, C.,  
754 Moutin, T. and Prieur, L.: Integrated survey of elemental stoichiometry (C, N, P) from the western to  
755 eastern Mediterranean Sea, *Biogeosciences*, 8(4), 883–899, doi:10.5194/bg-8-883-2011, 2011.

756 Sabine, C. L., Hoppema, M., Key, R. M., Tilbrook, B., Van Heuven, S., Lo Monaco, C., Metzl, N.,  
757 Ishii, M., Murata, A. and Musielewicz, S.: Assessing the internal consistency of the CARINA data  
758 base in the Pacific sector of the Southern Ocean, *Earth System Science Data Discussions*, 2(2), 195–  
759 204, doi:10.5194/essd-2-195-2010, 2010.

760 Schroeder, K., Tanhua, T., Bryden, H., Alvarez, M., Chiggiato, J. and Aracri, S.: Mediterranean Sea  
761 Ship-based Hydrographic Investigations Program (Med-SHIP), *Oceanography*, 28(3), 12–15,  
762 doi:10.5670/oceanog.2015.71, 2015.

763 Schroeder, K., Chiggiato, J., Bryden, H. L., Borghini, M. and Ben Ismail, S.: Abrupt climate shift in  
764 the Western Mediterranean Sea, *Scientific Reports*, 1–7, doi:10.1038/srep23009, 2016.Segura-  
765 Noguera, M., Cruzado, A. and Blasco, D.: The biogeochemistry of nutrients, dissolved oxygen and  
766 chlorophyll a in the Catalan Sea (NW Mediterranean Sea), *Sci. Mar.*, 80(S1), 39–56,  
767 doi:10.3989/scimar.04309.20a, 2016.

768 Segura-Noguera, M., Cruzado, A., & Blasco, D.: Nutrient preservation, analysis precision and quality  
769 control of an oceanographic database of inorganic nutrients, dissolved oxygen and chlorophyll a from  
770 the NW Mediterranean Sea. *Scientia Marina*, 75(2), 321-339, 2011.

771 Suzuki, T., Ishii, M., Aoyama, A., Christian, J. R., Enyo, K., Kawano, T., Key, R. M., Kosugi, N.,  
772 Kozyr, A., Miller, L. A., Murata, A., Nakano, T., Ono, T., Saino, T., Sasaki, K., Sasano, D., Takatani,  
773 Y., Wakita, M., and Sabine, C. L.: PACIFICA Data Synthesis Project, ORNL/CDIAC-159, NDP-092,

774 Carbon Dioxide Information Analysis Center, Oak Ridge National Laboratory, U. S. Department of  
775 Energy, Oak Ridge, Tennessee, 2013.

776 Tanhua, T.: Hydrochemistry of water samples during MedSHIP cruise Talpro. PANGAEA,  
777 <https://doi.org/10.1594/PANGAEA.902293>, 2019.

778 Tanhua, T.: Matlab Toolbox to Perform Secondary Quality Control (2nd QC) on Hydrographic Data,  
779 ORNL CDIAC-158. Carbon Dioxide Inf. Anal. Center, Oak Ridge Natl. Lab. U.S. Dep. Energy, Oak  
780 Ridge, Tennessee, 158, doi:10.3334/CDIAC/otg.CDIAC\_158, 2010a.

781 Tanhua, T., Brown, P. J. and Key, R. M.: CARINA : Nutrient data in the Atlantic Ocean, Earth  
782 Science Data, 1, 7–24, doi:10.3334/CDIAC/otg.CARINA.ATL.V1.0, 2009.

783 Tanhua, T., Heuven, S. van, Key, R. M., Velo, A., Olsen, A. and Schirnick, C.: Quality control  
784 procedures and methods of the CARINA database, Earth System Science Data, 2, 35–49, 2010b.

785 Tanhua, T., Hainbucher, D., Schroeder, K., Cardin, V., Álvarez, M. and Civitarese, G.: The  
786 Mediterranean Sea system: A review and an introduction to the special issue, Ocean Science, 9(5),  
787 789–803, doi:10.5194/os-9-789-2013, 2013.

788 Testor, P., Bosse, A., Houpert, L., Margirier, F., Mortier, L., Legoff, H., Dausse, D., Labaste, M.,  
789 Karstensen, J., Hayes, D., Olita, A., Ribotti, A., Schroeder, K., Chiggiato, J., Onken, R., Heslop, E.,  
790 Mourre, B., D’ortenzio, F., Mayot, N., Lavigne, H., de Fommervault, O., Coppola, L., Prieur, L.,  
791 Taillandier, V., Durrieu de Madron, X., Bourrin, F., Many, G., Damien, P., Estournel, C., Marsaleix,  
792 P., Taupier-Letage, I., Raimbault, P., Waldman, R., Bouin, M. N., Giordani, H., Caniaux, G., Somot,  
793 S., Ducrocq, V. and Conan, P.: Multiscale Observations of Deep Convection in the Northwestern  
794 Mediterranean Sea During Winter 2012–2013 Using Multiple Platforms, Journal of Geophysical  
795 Research: Oceans, 123(3), 1745–1776, doi:10.1002/2016JC012671, 2018.

796 Tintoré, J., Pinardi, N., Alvarez Fanjul, E., Balbin, R., Bozzano, R., Ferrarin, C.,... and Clementi, E.:  
797 Challenges for Sustained Observing and Forecasting Systems in the Mediterranean Sea. Frontiers in  
798 Marine Science, 6, 568, 2019.

799

800 **Figure Captions**

801 **Figure 1.** Map of the Western Mediterranean Sea showing the biogeochemical stations (in blue) and  
802 the five reference cruise stations (in red).

803 **Figure 2.** Overview of the reference cruise spatial coverage and vertical distributions of the inorganic  
804 nutrients. Top left: geographical distribution map, top right: vertical profiles of nitrate in  $\mu\text{mol kg}^{-1}$ ,  
805 bottom left: vertical profiles of phosphate in  $\mu\text{mol kg}^{-1}$ , bottom right: vertical profiles of silicate in  
806  $\mu\text{mol kg}^{-1}$ .

807 **Figure 3.** Scatter plots of (A.) phosphate vs nitrate (in  $\mu\text{mol kg}^{-1}$ ) and (B.) silicate vs. nitrate (in  $\mu\text{mol}$   
808  $\text{kg}^{-1}$ ). Data that have been flagged as “questionable” (flag=3) are in red, the colour bar indicates the  
809 pressure (in dbar). The black lines represent the best linear fit between the two parameters, and the  
810 corresponding equations and  $r^2$  values are shown on each plot. Average resulting N:P ratio is 20.87,  
811 average resulting N:Si ratio is 1.05 (whole depth).

812 **Figure 4.** An example of the calculated offset for silicate between cruise 48UR20131015 and cruise  
813 29AJ2016818 (reference cruise). Above: location of the stations being part of the crossover and  
814 statistics. Bottom left: vertical profiles of silicate data in ( $\mu\text{mol kg}^{-1}$ ) of the two cruises that fall within  
815 the minimum distance criteria (the crossing region), below 1000 dbar. Bottom right: vertical plot of  
816 the difference between both cruises (dotted black line) with standard deviations (dashed black lines)  
817 and the weighted average of the offset (solid red line) with the weighted standard deviations (dotted  
818 red line).

819 **Figure 5.** Results of the crossover analysis for nitrate, before (grey) and after adjustment (blue). Error  
820 bars indicate the standard deviation of the absolute weighted offset. The dashed lines indicate the  
821 accuracy limit 2% for an adjustment to be recommended.

822 **Figure 6.** The same as Fig. 5 but for phosphate.



823 **Figure 7.** The same as Fig. 5 but for silicate.

824 **Figure 8.** Dataset comparison before (black) and after (blue) adjustment, showing vertical profiles of  
825 (A.) nitrate (in  $\mu\text{mol kg}^{-1}$ ), (B.) phosphate (in  $\mu\text{mol kg}^{-1}$ ) and (C.) silicate (in  $\mu\text{mol kg}^{-1}$ ). Scatter plots  
826 of the adjusted data from all depths after 1<sup>st</sup> and 2<sup>nd</sup> quality control for (D.) phosphate vs nitrate (in  
827  $\mu\text{mol kg}^{-1}$ ) and (E.) silicate vs. nitrate (in  $\mu\text{mol kg}^{-1}$ ). The black lines represent the best linear fit  
828 between the two parameters, and the corresponding equations and  $r^2$  values are shown on each plot.  
829 Average resulting N:P ratio is 22.09, average resulting N:Si ratio is 0.94 (whole depth).

830 **Figure 9.** Vertical profiles of the inorganic nutrients in the dataset after adjustments and spatial  
831 coverage of each cruise (reference to cruise ID is above each map). The whole WMED adjusted  
832 product is shown in black while the data of each individual cruise are shown in blue (flag=2) and  
833 green (flag=3).

834 **Figure 10.** RMSE regional averages of water mass properties computed between the new adjusted  
835 product and MEDAR/Medatlas climatology for nitrate (A.), phosphate (B.) and silicate (C.).

836 **Table captions**

837 **Table 1a.** Cruise summary table and parameters listed with number of stations and samples. Cruises  
838 were identified with an ID number and expedition code ('EXPOCODE' of format  
839 AABBYYYMMDD with AA: country code, BB: ship code, YYYY: year, MM: month, DD: day  
840 indicative of cruise starting day).

841 **Table 1b.** Data sources and links to the reports (accessed June 2020).

842 **Table 2.** Cruise summary table of the reference cruises collection used in the secondary quality  
843 control, collected from 2001 to 2016.

844 **Table 3.** WOCE flags used in the original data product and in the adjusted product.

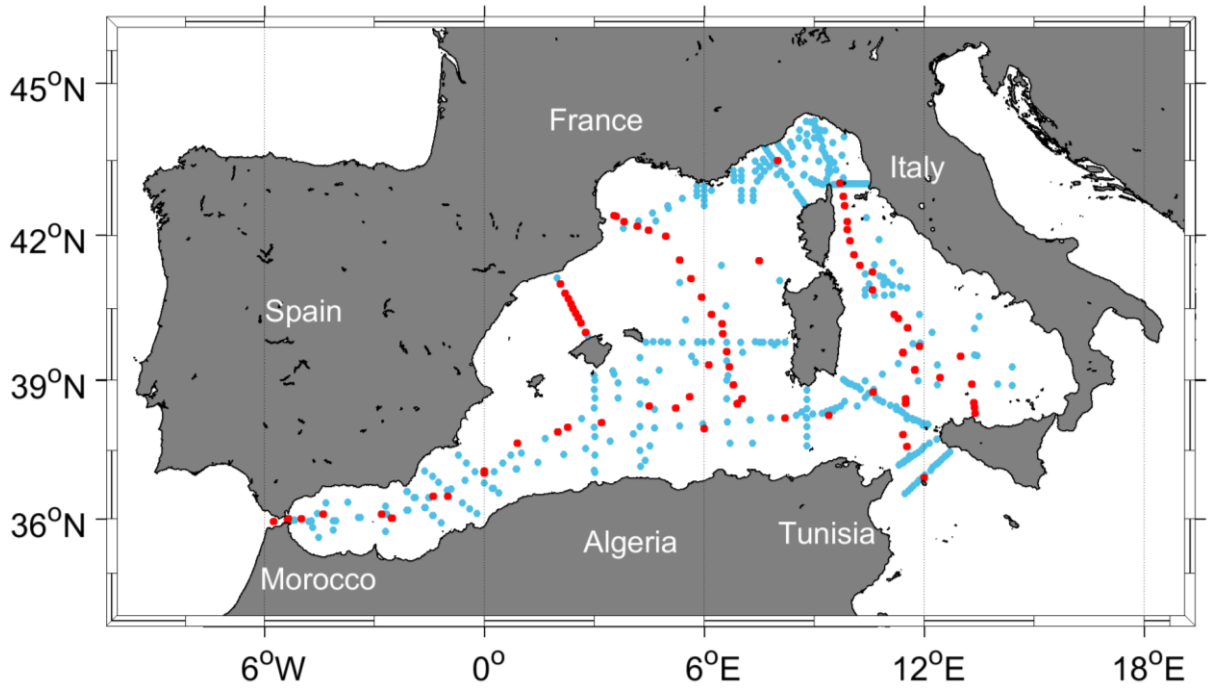
845 **Table 4.** Average and Standard deviations of nitrate, phosphate and silicate measurements by cruise  
846 and for each region with number of samples deeper than 1000db included in the 2<sup>nd</sup> QC. Average  
847 storage time: the minimum storage time defined as time difference between the cruise ending day and  
848 the 1<sup>st</sup> day of the laboratory analysis.

849 **Table 5.** Summary of the suggested adjustment for nitrate, phosphate and silicate resulting from the  
850 crossover analysis. Adjustments for inorganic nutrient are multiplicative. NA: denotes not adjusted,  
851 i.e. data of cruises that could not be used in the crossover analysis, because of the lack of stations or  
852 data are outside the spatial coverage of reference cruises.

853 **Table 6.** Secondary QC toolbox results: improvements of the weighted mean of absolute offset per  
854 cruise of unadjusted and adjusted data; (n) is the number of crossovers per cruise. The numbers in red  
855 (less than 1) indicate that the cruise data are lower than the reference cruises. NA: not adjusted.

856 **Table 7.** Water mass properties and regional average concentrations of inorganic nutrients:  
857 comparison between the new adjusted product and the MEDAR/Medatlas climatology (with standard  
858 deviations and number of observations in brackets).

859 **Figure 1**



860

861

862

863

864

865

866

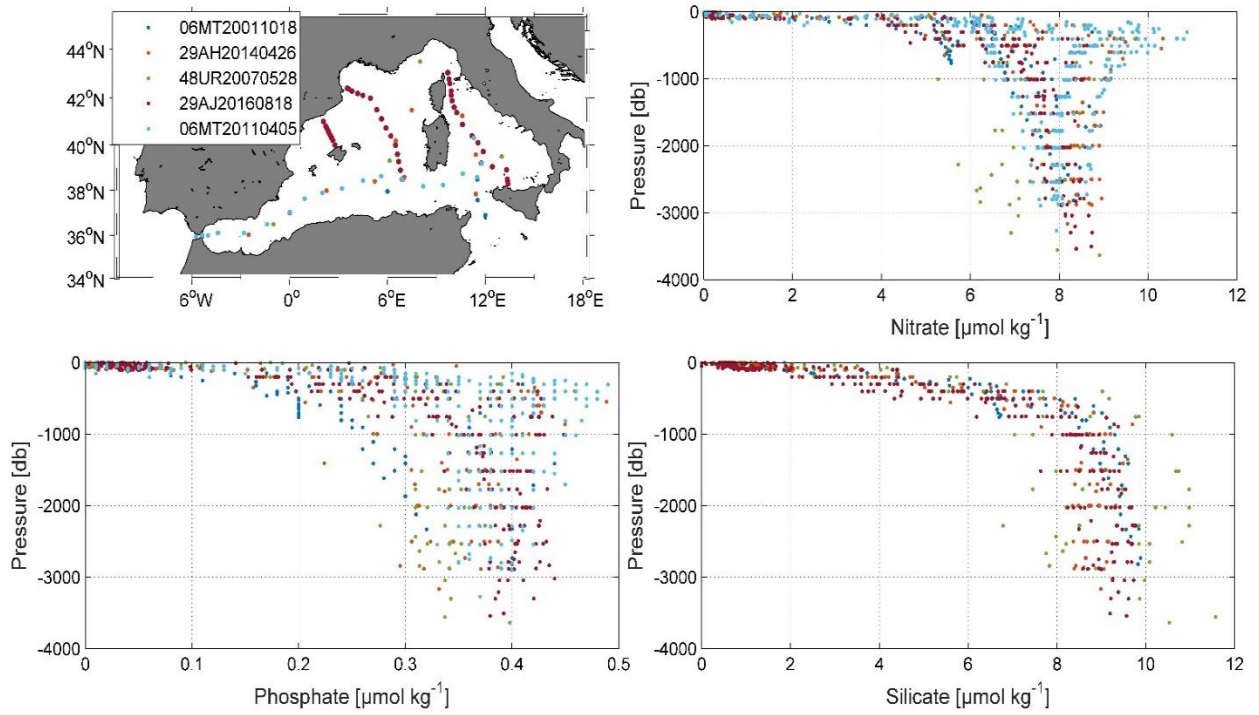
867

868

869

870

871 **Figure 2**



872

873

874

875

876

877

878

879

880

881

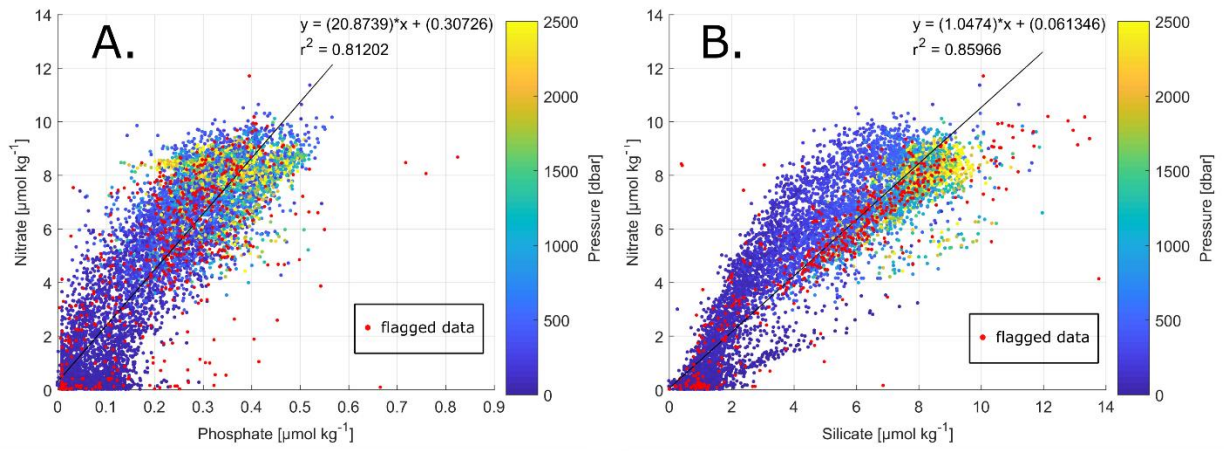
882

883

884

885

886 **Figure 3**



887

888

889

890

891

892

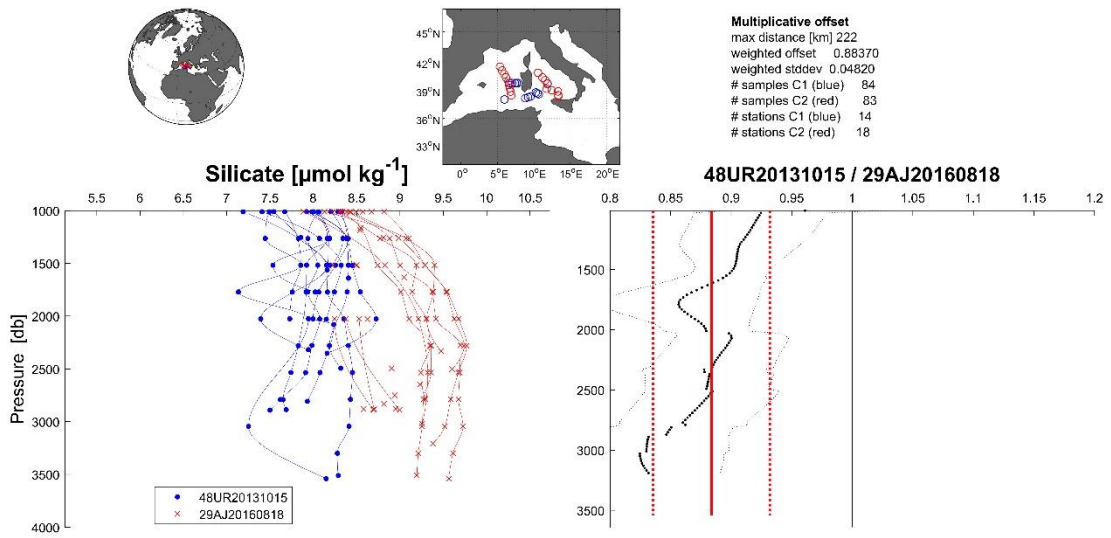
893 **Figure 4**

894

895

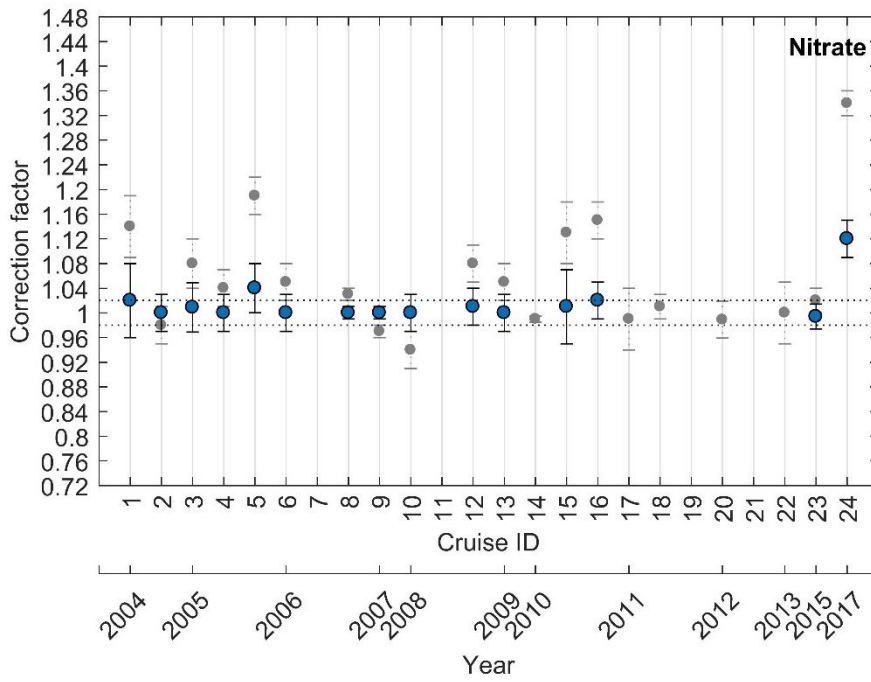
896

897



898

899 **Figure 5**



900

901

902

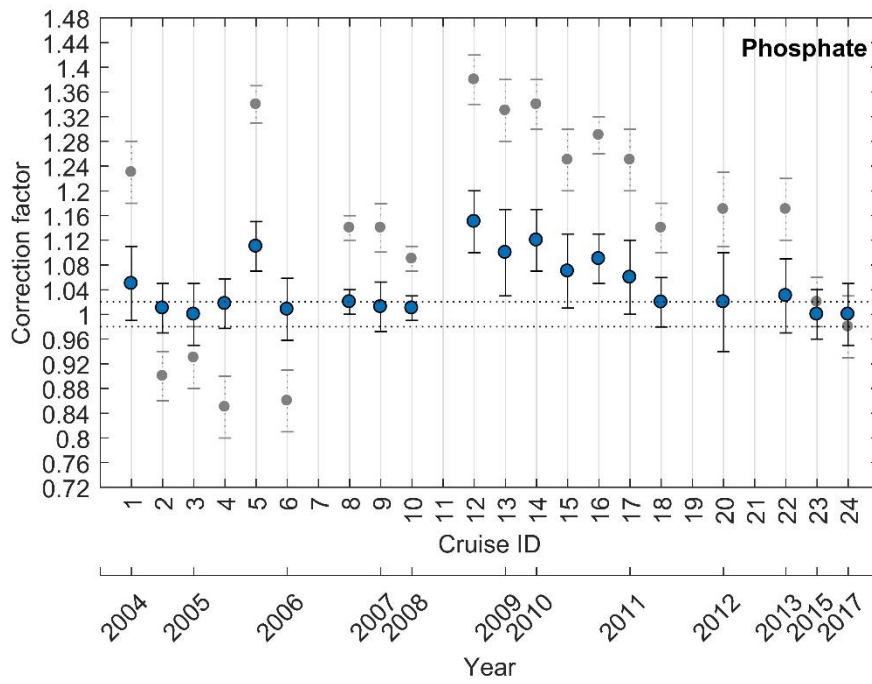
903

904

905

906  
907  
908  
909  
910  
911  
912  
913  
914  
915

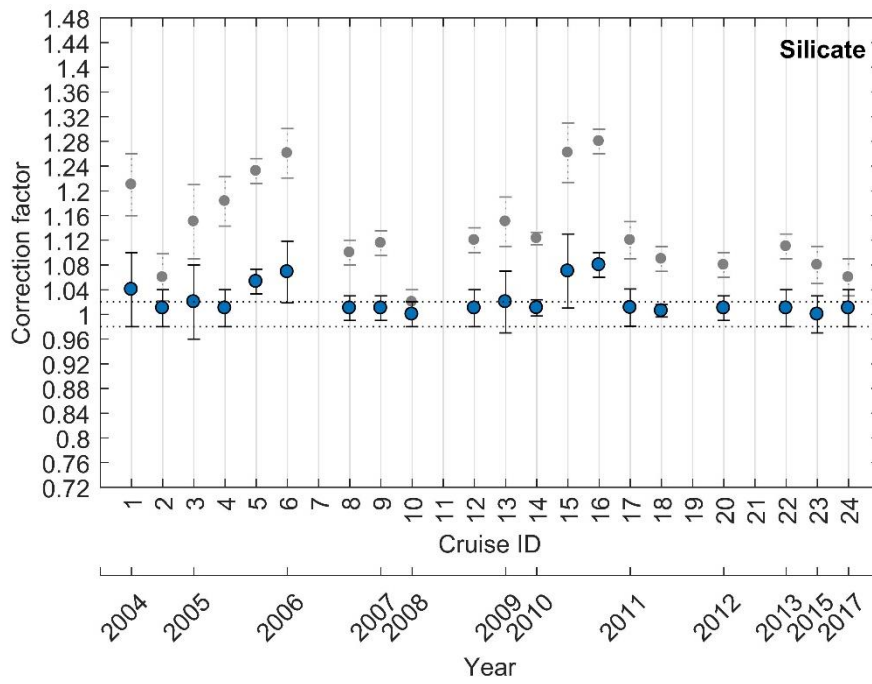
**Figure 6**



916  
917  
918  
919  
920  
921

922  
923  
924  
925  
926  
927  
928  
929  
930  
931

**Figure 7**

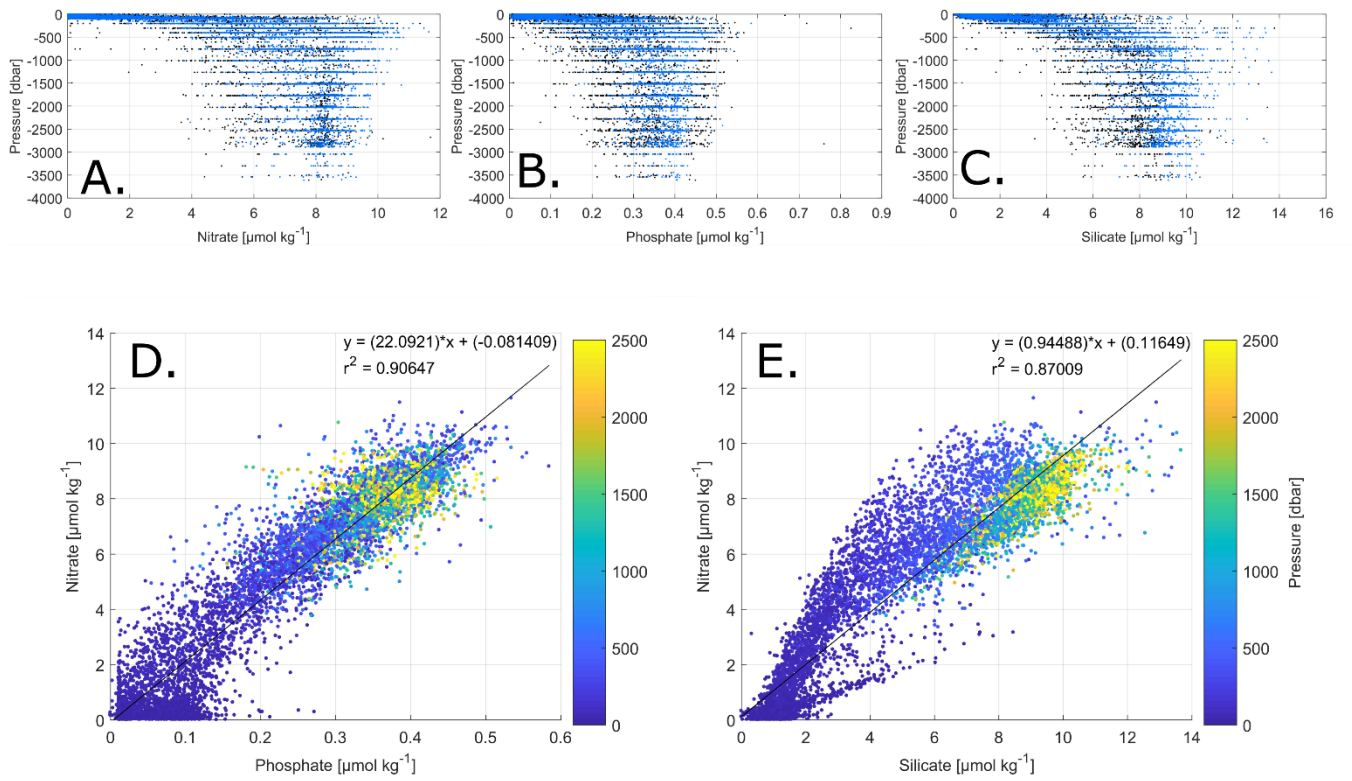


932  
933  
934  
935  
936  
937



938  
939  
940  
941  
942  
943  
944  
945  
946  
947

**Figure 8**



948  
949  
950  
951  
952

953

954

955

956

957

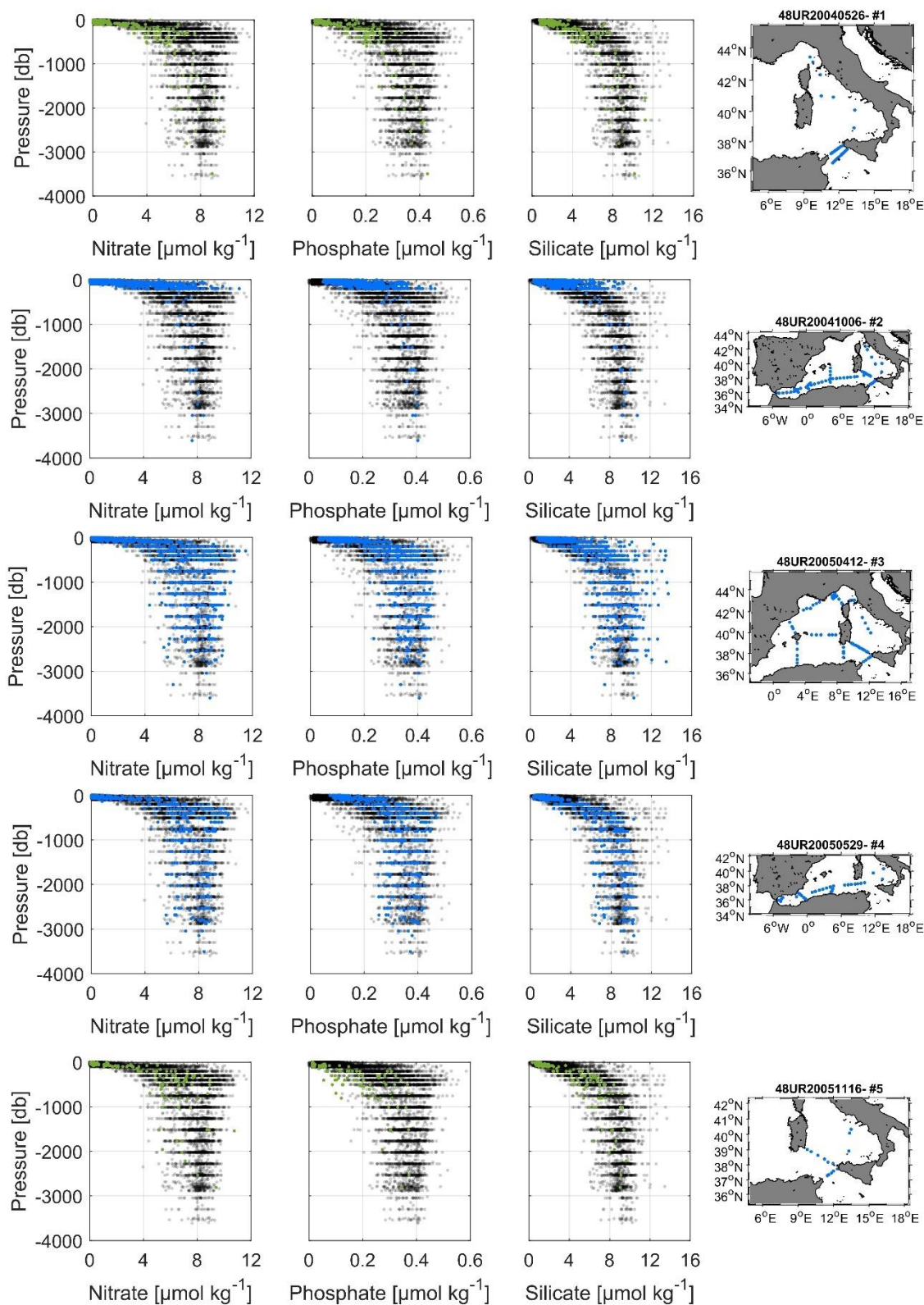
958

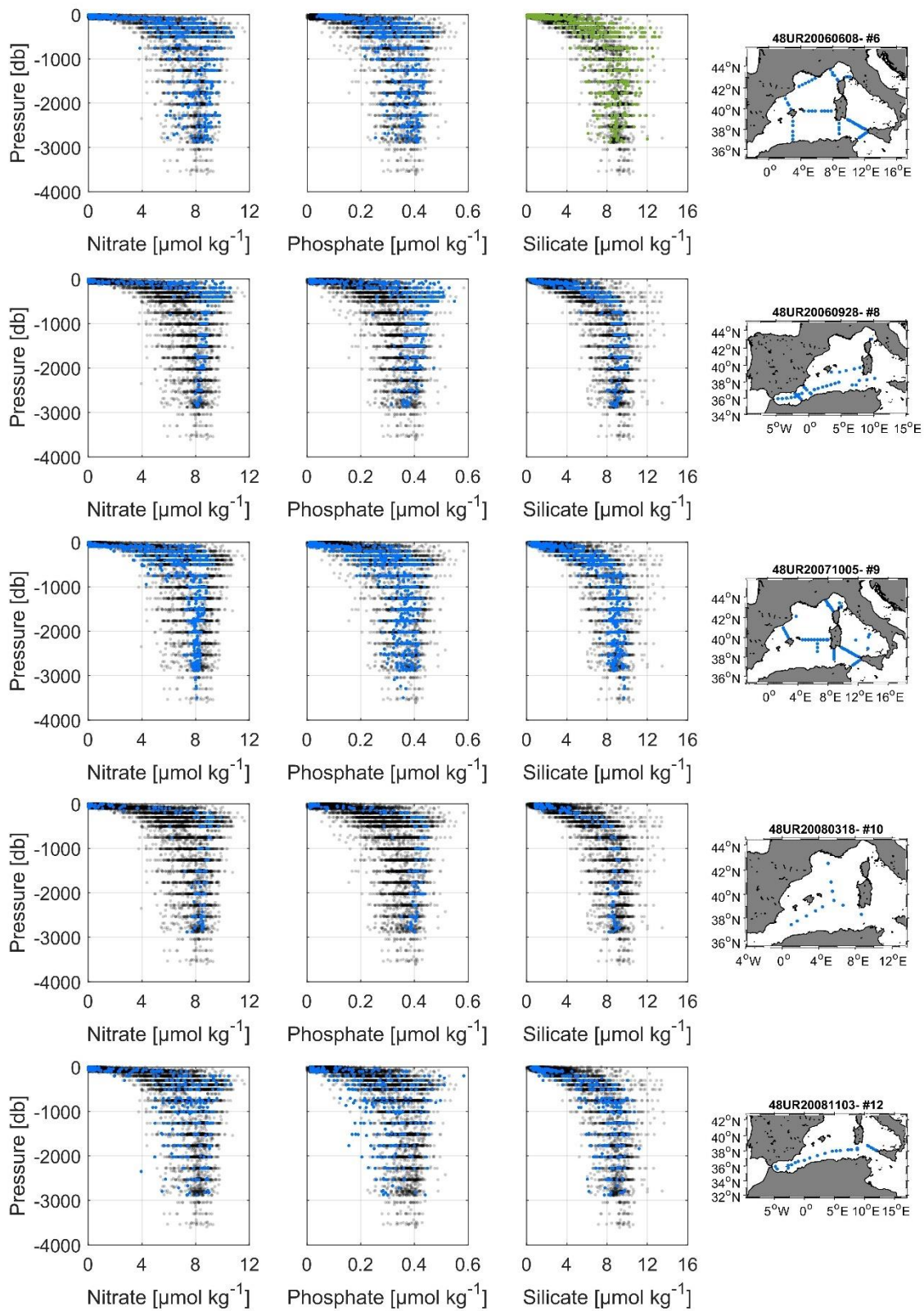
959

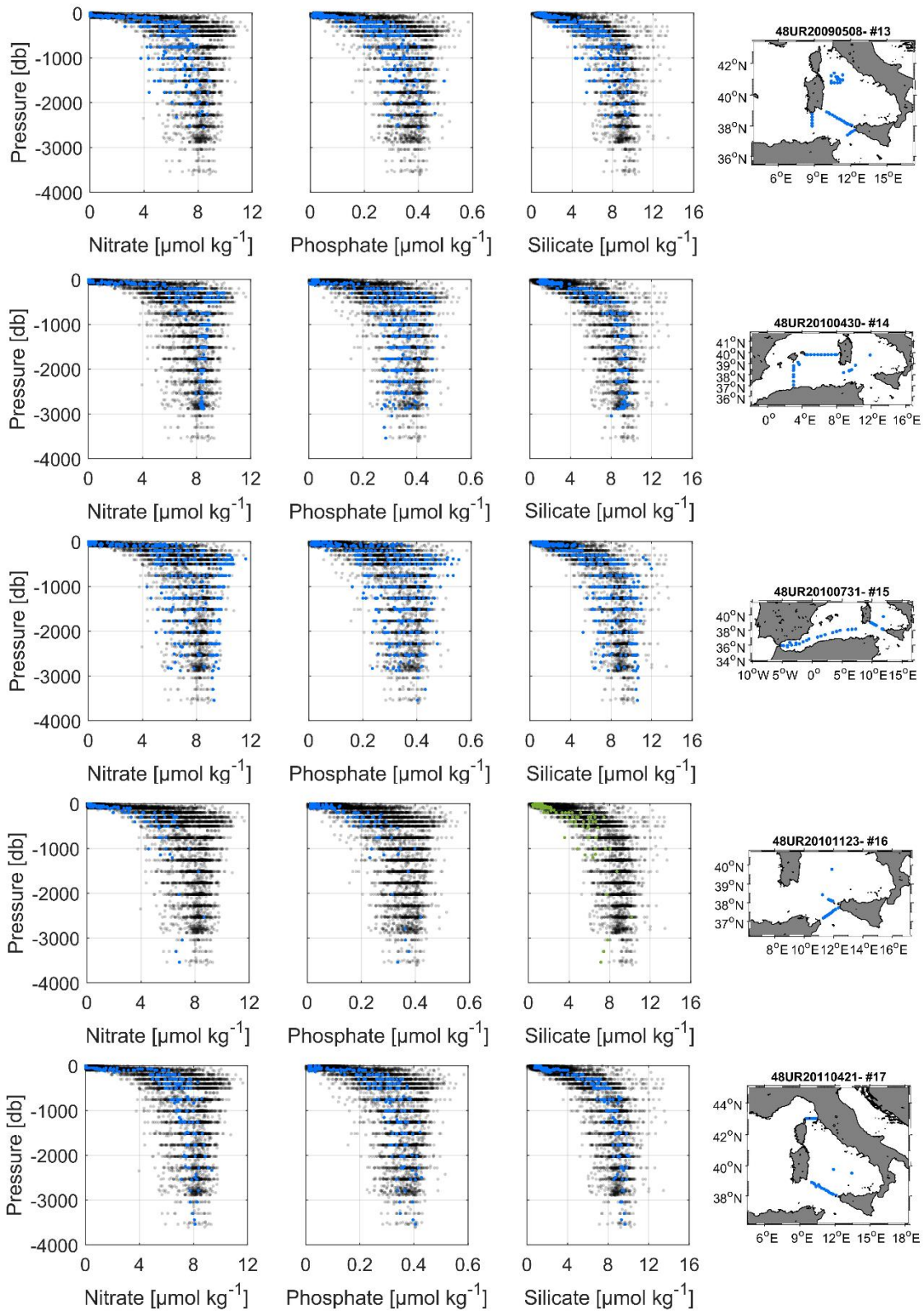
960

961

962 **Figure 9**

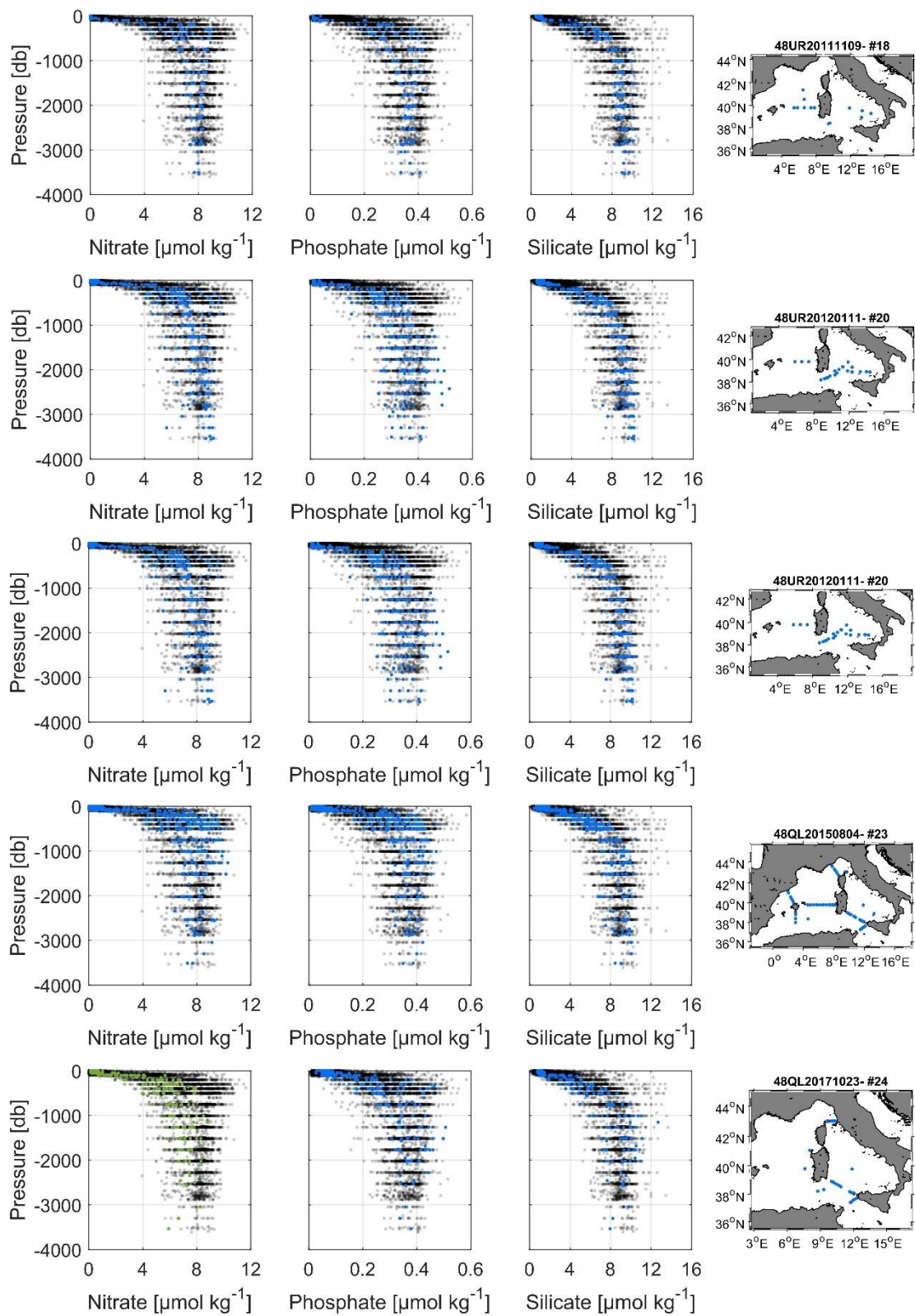






965

966

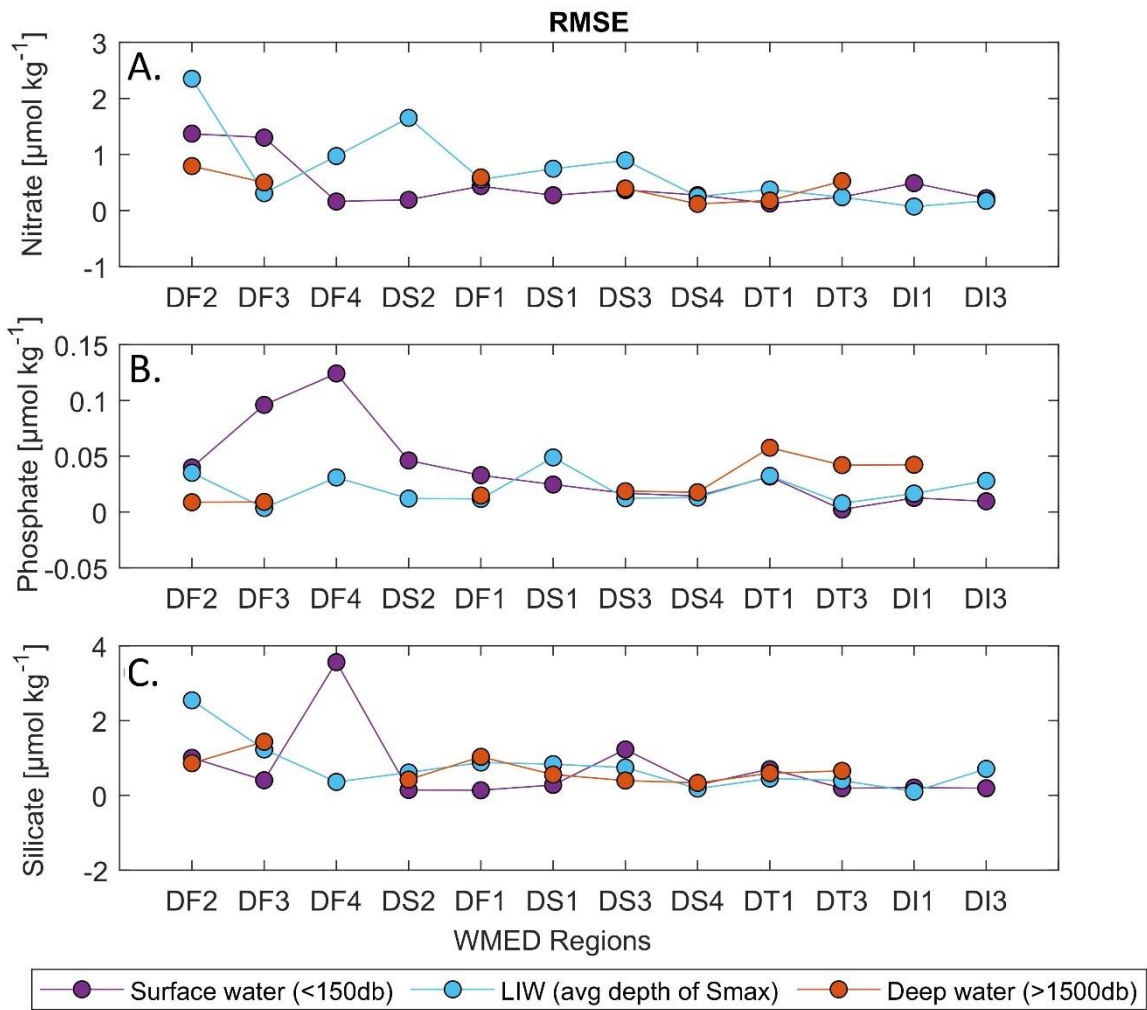


967

968

969 **Figure 10**

970



971

972

973

974

975

976

977

978

979

**Table 1a**

Cruise ID (#)	Common Name	EXPOCODE	Research vessel (RV)	Date Start/End	Stations	Samples Nitrate	Samples Phosphate	Samples Silicate	Maximum bottom depth (m)	Chief scientist
1	TRENDS2004/MEDGOOS8leg2	48UR20040526	Urania	26 MAY - 14 JUN 2004	36	255	253	255	3499	M. Borghini
2	MEDGOOS9	48UR20041006	Urania	6 - 25 OCT 2004	68	627	626	627	3610	M. Borghini
3	MEDOCC05/MFSTEP2	48UR20050412	Urania	12 APR - 16 MAY 2005	68	828	828	828	3598	M. Borghini
4	MEDGOOS10	48UR20050529	Urania	29 MAY - 10 JUN 2005	36	577	577	577	3505	A. Perilli
5	MEDGOOS11	48UR20051116	Urania	16 NOV - 3 DEC 2005	14	143	143	143	2810	A. Perilli, M. Borghini, M. Dibitto
6	MEDOCC06	48UR20060608	Urania	8 JUN - 3 JUL 2006	66	787	785	787	2881	M. Borghini
7	SIRENA06	06A420060720	NRV Alliance	20 JUL - 6 AUG 2006	35	208	208	209	1854	J. Haun
8	MEDGOOS13/MEDBIO06	48UR20060928	Urania	28 SEP - 8 NOV 2006	37	519	520	520	2862	A. Ribotti
9	MEDOCC07	48UR20071005	Urania	5 - 29 OCT 2007	71	977	977	979	3497	A. Perilli, M. Borghini
10	SESAMEIt4	48UR20080318	Urania	18 MAR - 7 APR 2008	11	164	164	164	2882	A. Ribotti
11	SESAMEIt5	48UR20080905	Urania	5 - 16 SEP 2008	12	74	74	74	536	C. Santinelli
12	MEDCO08	48UR20081103	Urania	3 - 24 NOV 2008	24	342	350	348	2880	S. Sparnocchia, G.P. Gasparini, M. Borghini
13	TYRRMOUNTS	48UR20090508	Urania	8 MAY - 3 JUN 2009	41	430	441	440	2559	A. Ribotti
14	BIOFUN010	48UR20100430	Urania	30 APR - 17 MAY 2010	26	405	405	405	3540	G.P. Gasparini
15	VENUS1	48UR20100731	Urania	31 JUL - 25 AUG 2010	32	431	432	428	3544	E. Manini, S. Aliani
16	BONSIC2010	48UR20101123	Urania	23 NOV - 9 DEC 2010	18	144	143	143	3540	G.P. Gasparini, M. Borghini
17	EUROFLEET11	48UR20110421	Urania	21 APR - 8 MAY 2011	28	277	275	277	3540	A. Ribotti
18	BONIFACIO2011	48UR20111109	Urania	9 - 23 NOV 2011	13	180	180	181	3541	G.P. Gasparini, M. Borghini
19	TOSCA2011	48MG20111210	Maria Grazia	10 - 20 DEC 2011	21	310	310	309	2728	A. Ribotti, G. La Spada, M. Borghini
20	ICHNUSSA12	48UR20120111	Urania	11 - 27 JAN 2012	21	353	352	323	3551	M. Borghini
21	EUROFLEET2012	48UR20121108	Urania	8 - 26 NOV 2012	53	429	434	434	2633	A. Ribotti
22	ICHNUSSA13	48UR20131015	Urania	15 - 29 OCT 2013	37	405	404	405	3540	J. Chiggiato
23	OCEANCERTAIN15	48QL20150804	Minerva Uno	4 - 29 AUG 2015	71	531	531	531	3513	A. Ribotti, S. Sparnocchia, M. Borghini
24	ICHNUSSA17/INFRAOCE17	48QL20171023	Minerva Uno	23 OCT - 28 NOV 2017	31	251	254	254	3536	



**Table 1b**

Cruise ID (#)	Expedition original Name	PIs/ Chief scientist	Specific link* (accessed June 2020)
1	TRENDS2004/ MEDGOOS8leg2	M. Borghini	<a href="https://isramar.ocean.org.il/perseus_data/CruiseInfo.aspx?criuseid=5821">https://isramar.ocean.org.il/perseus_data/CruiseInfo.aspx?criuseid=5821</a> <a href="https://isramar.ocean.org.il/perseus_data/CruiseInfo.aspx?criuseid=4935">https://isramar.ocean.org.il/perseus_data/CruiseInfo.aspx?criuseid=4935</a>
2	MEDGOOS9	M. Borghini	Report submission in progress <a href="https://isramar.ocean.org.il/perseus_data/CruiseInfo.aspx?criuseid=5823">https://isramar.ocean.org.il/perseus_data/CruiseInfo.aspx?criuseid=5823</a> <a href="https://doi.org/10.17882/70340">https://doi.org/10.17882/70340</a>
3	MEDOCC05/ MFSTEP2	M. Borghini	<a href="http://ricerca.ismar.cnr.it/CRUISE_REPORTS/2005/URANIA_MEDOCC05.pdf">http://ricerca.ismar.cnr.it/CRUISE_REPORTS/2005/URANIA_MEDOCC05.pdf</a> <a href="https://isramar.ocean.org.il/perseus_data/CruiseInfo.aspx?criuseid=4936">https://isramar.ocean.org.il/perseus_data/CruiseInfo.aspx?criuseid=4936</a>
4	MEDGOOS10	A. Perilli	<a href="http://www.seaforecast.cnr.it/it/observation_it.htm">http://www.seaforecast.cnr.it/it/observation_it.htm</a> <a href="https://doi.org/10.17882/70340">https://doi.org/10.17882/70340</a>
5	MEDGOOS11	A. Perilli, M. Borghini, M. Dibitetto	<a href="http://ricerca.ismar.cnr.it/CRUISE_REPORTS/2005/URANIA_MEDGOOS11_05_REP.pdf">http://ricerca.ismar.cnr.it/CRUISE_REPORTS/2005/URANIA_MEDGOOS11_05_REP.pdf</a> <a href="https://doi.org/10.17882/70340">https://doi.org/10.17882/70340</a>
6	MEDOCC06	M. Borghini	<a href="http://www.seaforecast.cnr.it/reports/Medocc06CR.pdf">http://www.seaforecast.cnr.it/reports/Medocc06CR.pdf</a> <a href="https://seadata.bsh.de/Cgi-csr/retrieve_sdn2/viewReport.pl?csrref=20106010">https://seadata.bsh.de/Cgi-csr/retrieve_sdn2/viewReport.pl?csrref=20106010</a>
7	SIRENA06	J. Haun	Report submission in progress
8	MEDGOOS13/ MEDBIO06	A. Ribotti	<a href="http://www.seaforecast.cnr.it/reports/Mebio06-Medg13_CR.pdf">http://www.seaforecast.cnr.it/reports/Mebio06-Medg13_CR.pdf</a> <a href="https://doi.org/10.17882/70340">https://doi.org/10.17882/70340</a>
9	MEDOCC07	A. Perilli, M. Borghini, A. Ribotti	<a href="http://www.seaforecast.cnr.it/reports/Medocc07-MedCo07_Rapp.pdf">http://www.seaforecast.cnr.it/reports/Medocc07-MedCo07_Rapp.pdf</a> <a href="https://isramar.ocean.org.il/perseus_data/CruiseInfo.aspx?criuseid=5146">https://isramar.ocean.org.il/perseus_data/CruiseInfo.aspx?criuseid=5146</a>
10	SESAMEIt4	C. Santinelli	<a href="https://isramar.ocean.org.il/perseus_data/CruiseInfo.aspx?criuseid=5148">https://isramar.ocean.org.il/perseus_data/CruiseInfo.aspx?criuseid=5148</a> <a href="https://emodnet-chemistry.maris.nl/search/details.php?step=0012004~0022017~0153~057104001~058tdin_ntra_phos_slca~00445~0056~00617~00734~0541&amp;count=3592&amp;page=1000&amp;sort=0&amp;header=no">https://emodnet-chemistry.maris.nl/search/details.php?step=0012004~0022017~0153~057104001~058tdin_ntra_phos_slca~00445~0056~00617~00734~0541&amp;count=3592&amp;page=1000&amp;sort=0&amp;header=no</a> <a href="https://isramar.ocean.org.il/perseus_data/CruiseInfo.aspx?criuseid=5147">https://isramar.ocean.org.il/perseus_data/CruiseInfo.aspx?criuseid=5147</a>
11	SESAMEIT5	S. Sparnocchia, G.P. Gasparini, M. Borghini	<a href="https://isramar.ocean.org.il/perseus_data/CruiseInfo.aspx?criuseid=5147">https://isramar.ocean.org.il/perseus_data/CruiseInfo.aspx?criuseid=5147</a>
12	MEDCO08	A. Ribotti	<a href="http://www.seaforecast.cnr.it/reports/MedCO08_Rapp.pdf">http://www.seaforecast.cnr.it/reports/MedCO08_Rapp.pdf</a>
13	TYRRMOUNTS	G.P. Gasparini	Report submission in progress
14	BIOFUN010	E. Manini, S. Aliani	<a href="http://www.ismar.cnr.it/products/reports-campagne/2010-2019">http://www.ismar.cnr.it/products/reports-campagne/2010-2019</a>
15	VENUS1	G.P. Gasparini, M. Borghini	Report submission in progress
16	BONSIC2010	A. Ribotti	<a href="http://www.seaforecast.cnr.it/reports/Bonifacio2010Sic_Rapp.pdf">http://www.seaforecast.cnr.it/reports/Bonifacio2010Sic_Rapp.pdf</a>
17	EUROFLEET11	G.P. Gasparini, M. Borghini	Report submission in progress
18	BONIFACIO2011	A. Ribotti, G. La Spada, M. Borghini	<a href="http://www.seaforecast.cnr.it/reports/Bonifacio2011_Rapp.pdf">http://www.seaforecast.cnr.it/reports/Bonifacio2011_Rapp.pdf</a>
19	TOSCA2011	M. Borghini	Report submission in progress
20	ICHNUSSA12	A. Ribotti	<a href="http://www.seaforecast.cnr.it/reports/Ichnussa2012_Rapp.pdf">http://www.seaforecast.cnr.it/reports/Ichnussa2012_Rapp.pdf</a>
21	EUROFLEET2012	M. Borghini	Report submission in progress
22	ICHNUSSA13	A. Ribotti	<a href="http://www.seaforecast.cnr.it/reports/Ichnussa2013_Rapp.pdf">http://www.seaforecast.cnr.it/reports/Ichnussa2013_Rapp.pdf</a>
23	OCEANCERTAIN15	J. Chiggiato	<a href="https://doi.org/10.1594/PANGAEA.911046">https://doi.org/10.1594/PANGAEA.911046</a>
24	ICHNUSSA17/ INFRAOCE17	A. Ribotti, S. Sparnocchia, M. Borghini	Report submission in progress

\* The specific links are subjected to updates.

**Table 2**

Common name	EXPOCODE	Date Start/End	Stations	Nitrate Sample	Phosphate Sample	Silicate Sample	Source	Nutrient PI	Chief scientist
<i>M51/2</i>	06MT20011018	18 OCT - 11 NOV 2001	6	79	79	82	GLODAPv2	B. Schneider	W. Roether
<i>TRANSMED_LEGII</i>	48UR20070528	28 MAY - 12 JUN 2007	4	78	77	78	CARIMED (not yet available)	S. Cozzi, V. Ibello	M. Azzaro
<i>M84/3</i>	06MT20110405	5 - 28 APR 2011	20	339	343	-	GLODAPv2	G. Civitarese	T. Tanhua
<i>HOTMIX</i>	29AH20140426	26 APR - 31 MAY 2014	18	144	140	144	CARIMED (not yet available)	XA Álvarez-Salgado	J. Aristegui
<i>TALPro-2016</i>	29AJ20160818	18 - 28 AUG 2016	42	293	293	293	MedSHIP programme	L. Coppola	L. Jullion, K. Schroeder

**Table 3**

WOCE flag value	Interpretation in original dataset	Interpretation in adjusted product
2	Acceptable/ measured	Adjusted and acceptable
3	Questionable/not used	Adjusted and recommended questionable
9	not measured/no data	-

**Table 4**

Cruise ID	EXPOCODE/ Region	Regional Avg Nitrate ( $\mu\text{mol}$ )	std Nitrate	Regional Avg Phosphate	std Phosphate(	Regional Avg Silicate ( $\mu\text{mol}$ )	std Silicate	# samples	Avg storage (in
-----------	------------------	--	-------------	------------------------	----------------	---	--------------	-----------	-----------------

		kg <sup>-1</sup> )	( $\mu\text{mol}$ kg <sup>-1</sup> )	( $\mu\text{mol}$ kg <sup>-1</sup> )	$\mu\text{mol}$ kg <sup>-1</sup> )	kg <sup>-1</sup> )	( $\mu\text{mol}$ kg <sup>-1</sup> )	days)	
1	48UR20040526/ <i>DT1-Tyrrhenian North</i> <i>DT3-Tyrrhenian South</i>	6.07 7.03	<b>1.25</b> 1.32 0.51	0.26 0.31	<b>0.062</b> 0.065 0.02	6.92 7.66	<b>1.64</b> 1.83 0.53	21 16 5	131
2	48UR20041006/ <i>DT1-Tyrrhenian North</i> <i>DT3-Tyrrhenian South</i>	7.68 8.17	<b>0.59</b> 0.53 0.60	0.41 0.41	<b>0.029</b> 0.031 0.025	8.74 9.31	<b>0.81</b> 0.75 0.87	21 15 6	251
3	48UR20050412/ <i>DF2-Gulf of Lion</i> <i>DF3-Liguro-Provençal</i> <i>DS2-Balearic Sea</i> <i>DF1-Algero-Provençal</i> <i>DS3-Algerian West</i> <i>DT1-Tyrrhenian North</i> <i>DT3-Tyrrhenian South</i> <i>DII-Sardinia Channel</i>	7.89 7.45 7.44 7.87 7.7 6.57 6.52 7.22	<b>1.15</b> 0.98 1.08 1.14 1.16 1.065 1.12 1.065	0.40 0.41 0.40 0.41 0.39 0.36 0.36 0.40	<b>0.050</b> 0.044 0.05 0.043 0.048 0.047 0.05 0.04	8.17 7.72 7.68 8.88 8.14 7.41 7.56 8.08	<b>1.41</b> 1.065 1.10 1.47 1.96 1.15 1.42 1.11	233 24 66 42 23 21 22 14	135
4	48UR20050529/ <i>DS1-Alboran Sea</i> <i>DS3-Algerian West</i> <i>DS4-Algerian East</i> <i>DT1-Tyrrhenian North</i> <i>DT3-Tyrrhenian South</i> <i>DII-Sardinia Channel</i>	6.4 7.6 7.48 7.24 7.70 7.58	<b>1.13</b> 1.15 1.13 1.13 0.44 0.38 1.08	0.38 0.41 0.41 0.42 0.41 0.43	<b>0.057</b> 0.041 0.06 0.06 0.03 0.049	6.26 7.33 7.50 7.91 7.55 7.42	<b>1.08</b> 1.02 0.99 1.23 0.56 0.82	205 32 73 16 14 23	314
5	48UR20051116/ <i>DT1-Tyrrhenian North</i> <i>DT3-Tyrrhenian South</i> <i>DII-Sardinia Channel</i>	5.68 6.71 6.29	<b>1.35</b> 1.26 1.51 0	0.19 0.20 0.26	<b>0.078</b> 0.08 0.06 0	6.30 6.86 7.53	<b>0.98</b> 0.92 1.065 0	16 10 5 1	738
6	48UR20060608/ <i>DF2-Gulf of Lion</i> <i>DF3-Liguro-Provençal</i> <i>DS2-Balearic Sea</i> <i>DF1-Algero-Provençal</i> <i>DS3-Algerian West</i> <i>DT3-Tyrrhenian South</i> <i>DII-Sardinia Channel</i>	7.69 8.08 8.06 7.97 8.39 6.39 8.04	<b>1.16</b> 1.02 0.78 0.9 1.16 0.9 0.85	0.42 0.43 0.43 0.44 0.42 0.36 0.43	<b>0.054</b> 0.04 0.04 0.03 0.05 0.03 0.04	7.089 7.41 7.07 7.34 8.5 6.86 7.77	<b>1.47</b> 1.04 1.21 1.18 1.32 2 1.7 1.25	221 27 35 30 61 28 26 14	27
7	06A420060720	-	-	-	-	-	-	-	1367
8	48UR20060928/ <i>DS2-Balearic Sea</i> <i>DF1-Algero-Provençal</i> <i>DS1-Alboran Sea</i> <i>DS3-Algerian West</i> <i>DS4-Algerian East</i> <i>DT3-Tyrrhenian South</i> <i>DII-Sardinia Channel</i>	7.97 8.17 8.2 7.93 7.98 6.2 7.66	<b>0.71</b> 0.17 0.22 0.14 0.89 0.68 1.51 0.6	0.33 0.33 0.35 0.33 0.34 0.28 0.28	<b>0.036</b> 0.017 0.026 0.02 0.03 0.04 0.02	7.84 8.11 8.59 8.09 8.01 6.71 8.00	<b>0.76</b> 0.27 0.3 0.35 0.91 0.7 1.45 0.49	179 4 22 47 70 3 5	606
9	48UR20071005/ <i>DF2-Gulf of Lion</i> <i>DF3-Liguro-Provençal</i> <i>DS2-Balearic Sea</i> <i>DF1-Algero-Provençal</i> <i>DS4-Algerian East</i> <i>DT1-Tyrrhenian North</i> <i>DT3-Tyrrhenian South</i> <i>DII-Sardinia Channel</i>	8.41 8.17 8.17 8.33 8.41 7.83 7.49 7.92	<b>0.89</b> 0.08 1.08 0.43 0.6 0.2 0.41 1.22 1.05	0.31 0.31 0.31 0.32 0.33 0.28 0.28 0.33	<b>0.040</b> 0.01 0.03 0.02 0.03 0.018 0.03 0.05 0.02	7.43 7.64 7.58 7.79 7.90 8.26 7.71 8.26	<b>0.86</b> 0.02 1.08 0.39 0.69 0.26 0.55 1.26 0.41	302 4 81 29 82 19 26 38 23	751
10	48UR20080318/ <i>DF2-Gulf of Lion</i> <i>DS2-Balearic Sea</i> <i>DF1-Algero-Provençal</i> <i>DS3-Algerian West</i> <i>DS4-Algerian East</i> <i>DII-Sardinia Channel</i>	8.54 9.12 9.02 8.93 8.43 7.62	<b>0.51</b> 0.6 0.18 0.36 0.46 0.25 0.6	0.35 0.38 0.38 0.36 0.38 0.34	<b>0.026</b> 0.03 0.01 0.03 0.01 0.02 0.03	8.62 8.40 8.65 8.69 8.32 8.49	<b>0.34</b> 0.43 0.21 0.25 0.35 0.22 0.36	66 5 9 15 20 10 3	31
11*	48UR20080905	-	-	-	-	-	-	-	211
12	48UR20081103/ <i>DS1-Alboran Sea</i> <i>DS3-Algerian West</i> <i>DS4-Algerian East</i> <i>DT3-Tyrrhenian South</i> <i>DII-Sardinia Channel</i>	6.4 7.58 7.15 7.44 7.40	<b>1.11</b> 1.21 0.9 1.04 0.5 1.23	0.21 0.27 0.23 0.22 0.17	<b>0.077</b> 0.06 0.1 0.04 0.05 0.04	7.20 7.89 7.38 8.28 8.09	<b>0.10</b> 1.43 0.9 0.9 0.45	110 26 30 10 9	536
13	48UR20090508/ <i>DT1-Tyrrhenian North</i> <i>DT3-Tyrrhenian South</i> <i>DII-Sardinia Channel</i>	5.95 6.76 7.62	<b>1.41</b> 1.55 0.77 1.1	0.24 0.24 0.28	<b>0.051</b> 0.05 0.03 0.05	6.28 7.37 7.76	<b>1.42</b> 1.58 0.77 0.9	88 46 29 13	164
14	48UR20100430/ <i>DS2-Balearic Sea</i> <i>DF1-Algero-Provençal</i>	7.66 8.43	<b>1.06</b> 1.6 0.29	0.25 0.26	<b>0.036</b> 0.03 0.03	7.38 8.06	<b>1.03</b> 1.75 0.31	159 33 61	213

	<i>DS3-Algerian West</i>	8.5	0.14	0.26	0.03	8.25	0.3	26	
	<i>DT1-Tyrrhenian North</i>	6.88	0.8	0.23	0.022	7.17	0.77	11	
	<i>DT3-Tyrrhenian South</i>	6.38	1.35	0.22	0.01	6.76	1.56	7	
	<i>DII-Sardinia Channel</i>	7.71	0.87	0.23	0.02	7.80	0.74	21	
15	48UR20100731/		<b>1.34</b>		<b>0.053</b>		<b>0.14</b>	149	213
	<i>DS1-Alboran Sea</i>	7.30	1.18	0.29	0.05	7.21	1.11	25	
	<i>DS3-Algerian West</i>	7.67	1.15	0.28	0.045	7.24	1.16	54	
	<i>DS4-Algerian East</i>	7.38	0.89	0.29	0.03	7.00	0.78	29	
	<i>DT1-Tyrrhenian North</i>	7.66	0.96	0.29	0.05	7.89	1.07	10	
	<i>DT3-Tyrrhenian South</i>	5.4	0.67	0.22	0.01	5.52	1.56	30	
	<i>DII-Sardinia Channel</i>	4.92	0	0.20	0	5.55	0	1	
16	48UR20101123/		<b>1.02</b>		<b>0.045</b>		<b>1.02</b>	14	170
	<i>DT1-Tyrrhenian North</i>	6.34	0.87	0.27	0.02	6.12	0.87	8	
	<i>DT3-Tyrrhenian South</i>	5.43	1.02	0.22	0.04	5.08	0.9	6	
17	48UR20110421/		<b>0.62</b>		<b>0.029</b>		<b>0.52</b>	56	160
	<i>DT1-Tyrrhenian North</i>	7.77	0.45	0.28	0.02	8.11	0.35	21	
	<i>DT3-Tyrrhenian South</i>	7.76	0.7	0.28	0.03	8.017	0.6	35	
18	48UR20111109/		<b>0.68</b>		<b>0.025</b>		<b>0.70</b>	77	74
	<i>DF3-Liguro-Provençal</i>	6.68	0	0.33	0	6.26	0	1	
	<i>DF1-Algero-Provençal</i>	8.17	0.5	0.32	0.01	8.16	0.66	43	
	<i>DT1-Tyrrhenian North</i>	7.26	0.93	0.29	0.02	8.15	1.03	12	
	<i>DT3-Tyrrhenian South</i>	7.61	0.37	0.30	0.02	8.18	0.35	11	
	<i>DII-Sardinia Channel</i>	7.64	0.45	0.29	0.01	8.08	0.41	10	
19*	48MG20111210		-		-		-	-	38
20	48UR20120111/		<b>0.97</b>		<b>0.051</b>		<b>0.26</b>	152	317
	<i>DF1-Algero-Provençal</i>	8.45	0.49	0.31	0.039	7.91	0.53	23	
	<i>DT1-Tyrrhenian North</i>	7.67	0.83	0.27	0.02	8.29	0.8	30	
	<i>DT3-Tyrrhenian South</i>	7.65	1.06	0.31	0.06	8.03	1.26	69	
	<i>DII-Sardinia Channel</i>	7.65	0.96	0.31	0.03	7.86	0.78	30	
21*	48UR20121108		-		-		-	-	72
22	48UR20131015/		<b>1.03</b>		<b>0.043</b>		<b>0.79</b>	98	76
	<i>DF1-Algero-Provençal</i>	8.54	0.64	0.33	0.02	7.96	0.38	36	
	<i>DS4-Algerian East</i>	7.67	1.28	0.27	0.04	6.82	1.07	8	
	<i>DT1-Tyrrhenian North</i>	6.47	0.83	0.24	0.025	7.12	0.84	10	
	<i>DT3-Tyrrhenian South</i>	7.81	0.71	0.30	0.03	8.09	0.65	28	
	<i>DII-Sardinia Channel</i>	7.32	0.99	0.27	0.02	7.47	0.89	16	
23	48QL20150804/		<b>0.84</b>		<b>0.038</b>		<b>0.85</b>	94	30
	<i>DF3-Liguro-Provençal</i>	8.51	0.96	0.39	0.03	8.06	0.85	23	
	<i>DS2-Balearic Sea</i>	7.75	0.66	0.36	0.02	7.86	0.81	20	
	<i>DF1-Algero-Provençal</i>	7.9	0.59	0.37	0.03	8.34	0.68	23	
	<i>DS3-Algerian West</i>	7.84	0.67	0.36	0.02	7.75	0.68	6	
	<i>DT1-Tyrrhenian North</i>	7.92	0.61	0.37	0.02	8.75	0.4	8	
	<i>DT3-Tyrrhenian South</i>	7.23	0.75	0.34	0.025	8.2	0.94	13	
	<i>DII-Sardinia Channel</i>	6.30	0	0.25	0	5.36	0	1	
24	48QL20171023/		<b>0.68</b>		<b>0.055</b>		<b>1.24</b>	55	30
	<i>DF3-Liguro-Provençal</i>	6.63	0.41	0.40	0.05	10.76	1.07	3	
	<i>DF1-Algero-Provençal</i>	5.14	0.7	0.43	0.02	7.94	1.19	6	
	<i>DT1-Tyrrhenian North</i>	4.98	0.58	0.36	0.02	8.10	0.87	9	
	<i>DT3-Tyrrhenian South</i>	5.43	0.5	0.36	0.04	9.03	0.87	26	
	<i>DII-Sardinia Channel</i>	5.16	0.76	0.41	0.07	7.58	1.17	11	

(\*) cruise not included in the 2<sup>nd</sup>QC (Section 4.)

in bold: the overall standard deviation by cruise; in normal font: regional standard deviation by cruise

**Table 5**

Cruise ID	EXPOCODE	Nitrate (x)	Phosphate (x)	Silicate (x)
1	48UR20040526	1.14	1.23	1.21
2	48UR20041006	0.98	0.9	1.06
3	48UR20050412	1.08	0.93	1.15
4	48UR20050529	1.04	0.85	1.183
5	48UR20051116	1.19	1.34	1.232

6	48UR20060608	1.05	0.86	1.261
7	06A420060720*	-	-	-
8	48UR20060928	1.03	1.14	1.1
9	48UR20071005	0.97	1.14	1.115
10	48UR20080318	0.94	1.09	1.02
11	48UR20080905*	-	-	-
12	48UR20081103	1.08	1.38	1.12
13	48UR20090508	1.05	1.33	1.15
14	48UR20100430	NA	1.34	1.123
15	48UR20100731	1.13	1.25	1.262
16	48UR20101123	1.15	1.29	1.28
17	48UR20110421	NA	1.25	1.12
18	48UR20111109	NA	1.14	1.09
19	48MG20111210*	-	-	-
20	48UR20120111	NA	1.17	1.08
21	48UR20121108*	-	-	-
22	48UR20131015	NA	1.17	1.11
23	48QL20150804	1.02	1.02	1.08
24	48QL20171023	1.34	0.98	1.06

(\*) cruise not included in the 2<sup>nd</sup>QC (Section 4.)

**Table 6**

Cruise ID	EXPOCODE	Nitrate [%]			Phosphate [%]			Silicate [%]		
		<i>n</i>	<i>unadjusted</i>	<i>adjusted</i>	<i>n</i>	<i>unadjusted</i>	<i>adjusted</i>	<i>n</i>	<i>unadjusted</i>	<i>adjusted</i>
1	48UR20040526	2	0.86	0.98	2	0.77	0.95	1	0.79	0.96
2	48UR20041006	2	1.02	1.00	2	1.10	0.99	1	0.94	0.99
3	48UR20050412	5	0.92	0.99	5	1.07	1.00	4	0.85	0.98
4	48UR20050529	5	0.96	1.00	5	1.15	0.98	4	0.82	0.99
5	48UR20051116	2	0.81	0.96	1	0.66	0.89	1	0.77	0.95
6	48UR20060608	5	0.95	1.00	5	1.14	0.99	4	0.74	0.93
7	06A420060720	0	-	-	0	-	-	0	-	-
8	48UR20060928	4	0.97	1.00	4	0.86	0.98	3	0.90	0.99
9	48UR20071005	5	1.03	1.00	5	0.86	0.98	4	0.88	0.99
10	48UR20080318	3	1.06	1.00	3	0.91	0.99	2	0.98	1.00
11	48UR20080905	0	-	-	0	-	-	0	-	-
12	48UR20081103	5	0.92	0.99	5	0.62	0.85	4	0.88	0.99
13	48UR20090508	3	0.95	1.00	3	0.67	0.90	2	0.85	0.98
14	48UR20100430	4	1.01	NA	4	0.66	0.88	3	0.88	0.99
15	48UR20100731	5	0.87	0.99	5	0.75	0.93	4	0.74	0.93
16	48UR20101123	1	0.85	0.98	1	0.71	0.91	1	0.72	0.92
17	48UR20110421	2	1.01	NA	2	0.75	0.94	1	0.88	0.99
18	48UR20111109	4	0.99	NA	4	0.86	0.98	3	0.91	0.99
19	48MG20111210	0	-	-	0	-	-	0	-	-
20	48UR20120111	4	1.01	NA	4	0.83	0.98	3	0.92	0.99
21	48UR20121108	0	-	-	0	-	-	0	-	-
22	48UR20131015	4	1.00	NA	4	0.83	0.97	3	0.89	0.99
23	48QL20150804	5	0.98	1.00	5	0.98	1.00	4	0.92	1.00
24	48QL20171023	3	0.66	0.88	3	1.02	1.00	2	0.94	0.99

red: data lower than reference

**Table 7**

Region/ Water mass	Nitrate ( $\mu\text{mol kg}^{-1}$ )		Phosphate ( $\mu\text{mol kg}^{-1}$ )		Silicate ( $\mu\text{mol kg}^{-1}$ )	
	Avg new Product	Avg Medar	Avg new Product	Avg Medar	Avg new Product	Avg Medar
<i>DF2- Gulf of Lion</i>						
surface water (0-150db)	2.68±2.53(68)**	1.7±1.1	0.15±0.06(68)	0.13±0.04	2.91±1.33(68)	1.72±0.64
LIW core ( $S_{\text{max}}$ depth range: 300-500db)	8.49±0.18(17)	6.13±0.32	0.38±0.02(17)	0.34±0.01	8.67±0.69(17)	6.12±0.61
Deep water (>1500db)	8.03±0.43(33)	7.64±0.31	0.37±0.01(33)	0.37±0.015	8.7±0.67(33)	7.95±0.06
<i>DF3- Liguro-Provençal</i>						
surface water (0-150db)	2.31±2.4(205)	3.0±2.6	0.12±0.07(205)	0.19±0.05	2.45±1.05(205)	2.16±1.05
LIW core ( $S_{\text{max}}$ depth range: 300-500db)	8.05±0.18(76)	7.74±0.13	0.36±0.01(76)	0.35±0.01	7.49±0.55(76)	6.26±0.60
Deep water (>1500db)	8.18±0.25(142)	7.79±0.04	0.37±0.02(142)	1.03±1.29	8.98±0.39(142)	7.60±0.21
<i>DF4- Ligurian East</i>						
surface water (0-150db)	0.7±0.69(228)	0.61±1.03	0.05±0.02(228)	0.18±0.02	1.37±0.45(228)	1.27±1.86
LIW core ( $S_{\text{max}}$ depth range: 300-500db)	6.8±0.4(23)	5.54±0	0.3±0.02(21)	0.36±0.06	5.86±0.9(24)	4.86±0
Deep water (>1500db)	-	-	-	-	-	-
<i>DS2- Balearic Sea</i>						
surface water (0-150db)	1.32±1.46(196)	1.19±1.5	0.08±0.04(196)	0.11±0.04	1.61±0.64(196)	1.54±0.78
LIW core ( $S_{\text{max}}$ depth range: 300-500db)	8.32±0.32(58)	6.92±0.12	0.37±0.02(60)	0.39±0.003	7.31±0.9(60)	7.55±0.62
Deep water (>1500db)	8.2±0.35(88)	-	0.37±0.01(88)	-	8.71±0.51(88)	8.45±0.8
<i>DF1- Algero-Provençal</i>						
surface water (0-150db)	0.87±0.85(372)	1.08±1.7	0.05±0.02(372)	0.07±0.05	1.42±0.3(372)	1.28±0.73
LIW core ( $S_{\text{max}}$ depth range: 300-500db)	8.07±0.34(126)	7.51±0.18	0.36±0.02(126)	0.34±0.008	6.84±0.95(126)	5.96±0.77
Deep water (>1500db)	8.36±0.27(300)	7.87±0.13	0.38±0.02(300)	0.38±0.001	9.01±0.33(300)	8.18±0.10
<i>DS1- Alboran Sea</i>						
surface water (0-150db)	2.75±2.87(299)	2.51±2.23	0.17±0.11(299)	0.16±0.07	2.07±1.38(299)	2.31±1.14
LIW core ( $S_{\text{max}}$ depth range: 400-600db)	8.89±0.4(77)	8.14±0.11	0.42±0.02(77)	0.37±0.008	8.77±1.66(76)	7.95±0.34
Deep water (>1500db)	7.72±0.81(65)	-	0.36±0.04(65)	-	8.98±0.63(65)	8.16±0
<i>DS3- Algerian West</i>						
surface water (0-150db)	1.8±1.88(254)	1.82±2.01	0.11±0.05(354)	0.11±0.06	1.71±0.68(354)	2.10±0.91
LIW core ( $S_{\text{max}}$ depth range: 400-600db)	9.33±0.08(70)	8.28±0.15	0.41±0(73)	0.38±0.012	8.1±0.53(72)	6.68±0.80
Deep water (>1500db)	8.37±0.27(246)	8.047±0.013	0.37±0.02(246)	0.36±0.006	9.22±0.35(246)	8.87±0.23
<i>DS4- Algerian East</i>						
surface water (0-150db)	0.94±0.77(170)	0.75±1.26	0.07±0.02(170)	0.05±0.03	1.53±0.12(170)	1.35±0.52
LIW core ( $S_{\text{max}}$ depth range: 400-600db)	8.5±0.25(43)	8.60±0.06	0.38±0.03(43)	0.38±0.008	7.27±0.67(42)	7.092±0.55
Deep water (>1500db)	7.94±0.24(132)	8.06±0.06	0.36±0.02(132)	0.38±0.006	8.73±0.38(132)	9.04±0.24
<i>DT1- Tyrrhenian North</i>						
surface water (0-150db)	1.03±1.14(231)	0.88±1.2	0.06±0.02(231)	0.09±0.03	1.64±0.52(231)	2.19±0.59
LIW core ( $S_{\text{max}}$ depth range: 400-600db)	5.95±0.49(43)	5.86±0.36	0.27±0.03(44)	0.308±0.02	7.06±0.08(44)	6.76±0.59
Deep water (>1500db)	7.75±0.37(194)	7.12±0.47	0.36±0.03(194)	0.40±0.02	9.19±0.47(194)	7.51±0.49
<i>DT3- Tyrrhenian South</i>						
surface water (0-150db)	1.21±1.38(711)	1.23±1.80	0.06±0.03(711)	0.061±0.04	1.58±0.61(711)	1.55±1.05
LIW core ( $S_{\text{max}}$ depth range: 300-500db)	6.2±0.28(225)	6.42±0.01	0.26±0.02(225)	0.254±0.005	6.28±0.65(224)	6.68±0.44
Deep water (>1500db)	7.88±0.4(227)	7.12±0.26	0.37±0.02(227)	0.31±0.007	9.04±0.52(227)	8.02±0.07
<i>DII- Sardinia Channel</i>						
surface water (0-150db)	1.22±1.39(271)	1.42±1.95	0.07±0.03(271)	0.064±0.03	1.57±0.68(271)	1.39±1.01
LIW core ( $S_{\text{max}}$ depth range: 300-500db)	6.52±0.17(89)	6.45±0.22	0.27±0.02(89)	0.250±0.01	6.36±0.67(89)	6.27±0.70
Deep water (>1500db)	7.91±0.62(107)	-	0.37±0.03(107)	0.32±0	8.64±0.91(107)	-
<i>DI3- Sicily Strait</i>						
surface water (0-150db)	0.87±0.68(583)	0.77±0.81	0.06±0.02(583)	0.063±0.02	1.53±0.29(583)	1.44±0.58
LIW core ( $S_{\text{max}}$ depth range: 200-400db)	4.95±0.47(80)	5.14±0.14	0.21±0.02(78)	0.194±0.004	5.26±0.79(81)	6.744±0.41
Deep water (>1500db)	-	-	-	-	-	-

\*\*Average (Avg) ± standard deviation of inorganic nutrient (the number observation within depth range) for three layers from the adjusted/new product and MEDATLAS vertical climatological profiles (called here Medar). Regions are defined according to Manca et al. (2004) (table 2S, Fig.2S)